JOURNAL OF GUIDANCE, CONTROL, AND DYNAMICS
Vol. 33, No. 3, May–June 2010

Electric Sail Mission Analysis for Outer Solar System Exploration

Alessandro A. Quarta* and Giovanni Mengali†
University of Pisa, Pisa 56122 Italy

DOI: 10.2514/1.47006

Missions toward the boundaries of the solar system require long transfer times and advanced propulsion systems. An interesting option is offered by electric sails, a new propulsion concept that uses the solar wind dynamic pressure for generating a continuous thrust without the need for reaction mass. The aim of this paper is to investigate the performance of such a propulsion system for obtaining escape conditions from the solar system and planning a mission to reach the heliosphere boundaries. The problem is studied in an optimal framework by minimizing the time to reach a given solar distance or a given hyperbolic excess speed. Depending on the value of the sail characteristic acceleration, it is possible that, in an initial mission phase, the sailcraft may approach the sun to exploit the increased available thrust due to the growing solar wind electron density. The corresponding optimal trajectory is constrained to not pass inside a heliocentric sphere for which the admissible radius is established by thermal constraints. Once the escape condition is met, the sail is jettisoned and the payload alone continues its journey without any primary propulsion system. A medium-performance electric sail is shown to have the potentialities to reach the heliosheath, at a distance of 100 astronomical unit from the sun, in about 15 years. Finally, the Interstellar Heliopause Probe mission is used as a reference mission to further quantify the electric sail capabilities for an optimal transfer toward the heliopause nose (200 astronomical unit).

Nomenclature

a	=	initial orbit semimajor axis
$a_\oplus$	=	sailcraft characteristic acceleration
$\boldsymbol{a}_p$	=	propelling acceleration, $a_p \triangleq \|\boldsymbol{a}_p\|$
$\mathcal{E}$	=	mechanical specific energy
e	=	initial orbit eccentricity
F	=	maximum propelling thrust at $r = r_\oplus$
H	=	Hamiltonian
J	=	performance index
k_P	=	power subsystem mass margin
k_s	=	structure mass margin
L	=	total tethers length
l	=	tether length
m_E	=	electric sail mass
m_P	=	power subsystem mass
m_p	=	platform mass
m_s	=	structure mass
m_{th}	=	tethers total mass
m_0	=	sailcraft in-flight total mass
n	=	tethers number
P	=	electron gun power
r	=	sun-sailcraft distance, $r_\oplus \triangleq 1$ AU
$\mathcal{T}_\odot(r, \psi, \phi)$	=	inertial spherical reference frame
$\mathcal{T}_\odot(r, \theta)$	=	inertial polar reference frame
t	=	time
u	=	radial component of velocity
V	=	sailcraft final velocity modulus
V_∞	=	hyperbolic excess speed
v	=	circumferential component of velocity
α	=	sail cone angle
α_λ	=	primer vector cone angle
δ	=	sail clock angle
η	=	specific power
θ	=	polar angle
λ_i	=	adjoint variable, with $i = r, \theta, u, v$
$\mu_\odot$	=	sun's gravitational parameter
σ_F	=	propelling thrust density
$\sigma_{m_{\text{th}}}$	=	tethers mass density
σ_P	=	electron gun power density
τ	=	switching parameter
ϕ	=	ecliptic latitude
ψ	=	ecliptic longitude

Subscripts

c	=	cutoff
H	=	heliopause nose
max	=	maximum
min	=	minimum
on	=	electric sail on
0	=	initial
1	=	perihelion
2	=	final
100	=	100 AU

Superscripts

$\bar{\ }$	=	mean over $\theta_0 \in [0, 2\pi]$
$\dot{\ }$	=	time derivative

Introduction

THE scientific importance of sending a spacecraft to the outer solar system (SS) boundaries is widely accepted as the primary means to obtain a more comprehensive knowledge of the heliosphere and the nearby interstellar medium. A number of key open questions about those unexplored regions exist as, for example, the distribution of matter in the outer SS, the chemical evolution of our galaxy, the structure and dynamics of the heliosphere, and the nature and properties of the nearby galactic medium. Currently, only two spacecraft, Voyager 1 and 2, having reached the SS boundaries, are capable of obtaining in situ information. Voyager 1 crossed the termination shock (in which the solar wind speed changes from being supersonic to subsonic) on December 2004, at a distance of 94 astronomical unit (AU) from the sun, becoming the first spacecraft to begin exploring the heliosheath, the outermost layer of the heliosphere [1]. Voyager 2 has performed several crossings of the termination shock between 30 August and 1 September 2007. Since

Received 3 Sept. 2009; accepted for publication 28 Oct. 2009.

*Research Assistant, Department of Aerospace Engineering; a.quarta@ing.unipi.it. Senior Member AIAA.

†Associate Professor, Department of Aerospace Engineering; g.mengali@ing.unipi.it. Senior Member AIAA.

then, Voyager 2 has remained in the heliosheath [2]. Although Voyager 1 and 2 are making fundamental discoveries, their instruments were designed to investigate the outer planets and their satellites. Therefore, there are many properties that Voyager's 30 year old instruments are unable to measure. New missions are necessary, with specifically designed instruments, to make comprehensive measurements and deepen human knowledge of the SS boundaries.

Those very long distances from the sun, about 100–200 AU, take a long time to be reached using conventional (chemical) or advanced (solar and nuclear electric) propulsion technology, even when combined with planetary and solar gravity assists [3]. Therefore, a primary requirement of new missions is the use of exotic propulsion systems. Not surprisingly, several recent mission studies toward the heliospheric boundaries and the nearby interstellar space are based on the employment of solar sails [4,5]. Until now, solar sailing has proven to be the only feasible solution to reach the heliopause nose, at a distance of about 200 AU, with a flight time of 25 years and a final SS escape velocity of about 10 AU/year [6,7]. In fact, neglecting the degradation effects of the sail reflective film [8–10] caused by the interactions with the solar light, solar sails can provide a continuous thrust for the whole mission length and gain a large amount of ΔV in a reasonable time through a close approach to the sun [5,11,12].

Excluding the minimagnetospheric plasma propulsion (M2P2) [13–16], which requires a certain amount of propellant to create a large magnetic plasma bubble around the spacecraft, those previous characteristics were, until recently, a prerogative of solar sails alone. Currently an alternative exists, because the electric sail [17] is theoretically capable of fulfilling similar requirements for missions toward the SS boundaries. The electric sail is an innovative propulsion concept that uses the solar wind dynamic pressure for generating a thrust without the need for reaction mass [17–19]. The spacecraft is spun around a symmetry axis and uses the centrifugal force to deploy and stretch out a number of thin, long, conducting tethers [20]. The latter are held at high positive potential by an electron gun, for which the electron beam is shot roughly along the spin axis. The resulting static electric field of the tethers perturbs the trajectories of the incident solar wind protons, thus producing a momentum transfer from the solar wind plasma stream to the tethers.

The electric sail thrust concept has been used to calculate successful and efficient mission trajectories in the SS for realistic payloads [20–22]. However, a detailed study regarding the feasibility of reaching the SS boundaries has not yet been performed. The aim of this paper is to provide alternative results and preliminary mission studies using an electric sail as a primary propulsion system. In particular, a key point is to investigate whether an electric sail is suitable for reaching either the heliosheath or the heliopause nose in a reasonable flight time and with a launch mass comparable to that required by a solar sail based option.

The paper is organized as follows. First, the electric sail minimum-time performance, necessary to reach a given hyperbolic excess speed with respect to the SS, is studied in a 2-D framework. This analysis provides preliminary information on the effect of a close approach to the sun (to increase the sailcraft available thrust) on an escape mission from the SS. Then, the minimum flight times required to reach a prescribed distance from the sun is calculated using a 2-D model. Such information is employed as a starting point for a 3-D analysis of the problem, which takes into account the actual position of the heliopause nose. Finally, the obtained results are used, with the aid of a suitable mass distribution model, to get an estimate of the sailcraft mass characteristics.

Problem Description

Consider an electric sail placed on a heliocentric elliptic orbit with given values of semimajor axis a and eccentricity e, and let r_0 be the sailcraft distance from the sun at the initial time t_0. The electric sail trajectory for $t > t_0$ is studied with the aid of a heliocentric polar reference frame $\mathcal{T}_\odot(r, \theta)$, where the polar angle θ is measured anticlockwise from a fixed direction. The generic sailcraft trajectory, illustrated in Fig. 1, may include a close approach to the sun for increasing the sailcraft propelling acceleration. However, the sun-sailcraft distance cannot decrease below a minimum admissible value $r_{\min}$ imposed by thermal constraints.

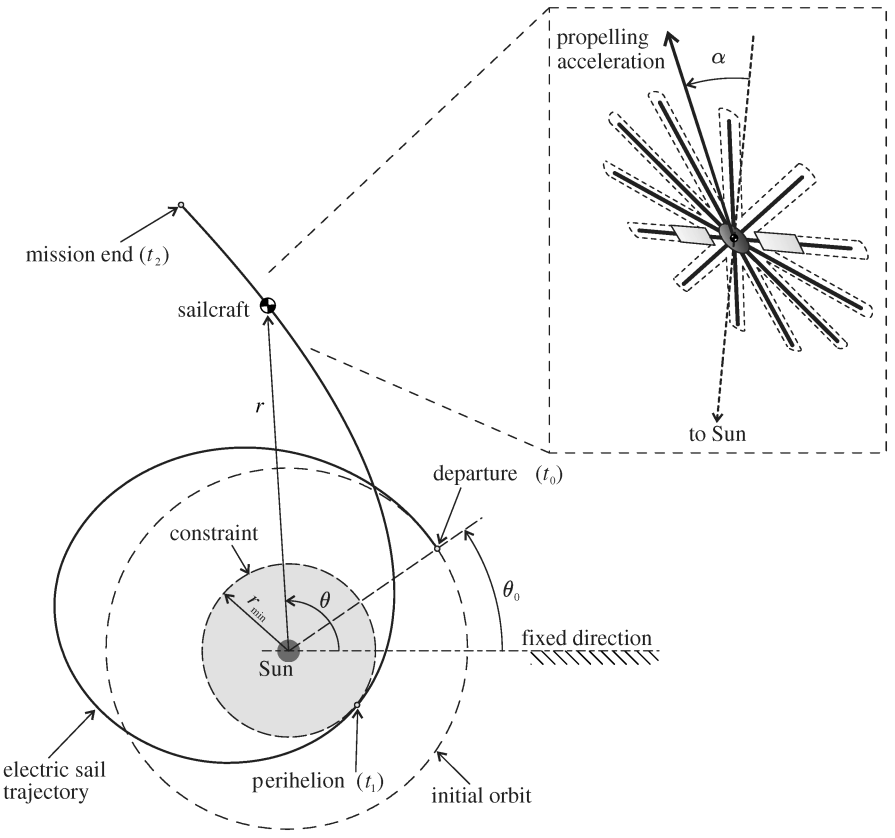

Fig. 1 Polar reference frame and typical electric sail 2-D trajectory.

In a first phase of this study assume a 2-D problem in which the orbital plane coincides with the ecliptic plane. This allows one to obtain a first estimate of the electric sail minimum-time performance for a number of mission scenarios in a reduced computational time. Let t_1 be the time instant in which the sailcraft reaches the minimum distance from the sun, and t_2 the time of mission end (total flight time). The problem addressed here is to minimize the time t_2 necessary to transfer the spacecraft from an initial given state $[r(t_0), \theta(t_0), u(t_0), v(t_0)]$ to a final prescribed state $[r(t_2), \theta(t_2), u(t_2), v(t_2)]$. This amounts to maximizing the scalar performance index:

$$J = -t_2 \tag{1}$$

The electric sail trajectory may be tuned through two independent control variables, τ and α [20,23]. The switching parameter $\tau = (0, 1)$ models the thruster on/off condition, and is introduced to account for coasting arcs in the spacecraft trajectory. The second control variable, that is, the sail cone angle α, coincides with the angle between the sun-sailcraft line and the thrust direction, see Fig. 1. The value of α may be adjusted in the range $[-\alpha_{\max}, \alpha_{\max}]$ by suitably orienting the plane containing the sail tethers as described in Mengali et al. [20].

The electric sail propelling acceleration modulus depends on the sailcraft distance from the sun as [20,23]

$$a_p = a_\oplus \left(\frac{r_\oplus}{r}\right)^{7/6} \tag{2}$$

where $a_\oplus$, referred to as sail characteristic acceleration (in analogy to the solar sail case), is the maximum propelling acceleration at $r = r_\oplus \triangleq 1$ AU. Accordingly, $a_\oplus$ is the parameter commonly used to quantify the electric sail performance. The problem of maximizing the performance index J may be addressed with an indirect approach, and its solution is described elsewhere [20]. In particular, four scalar first-order differential equations are necessary to describe the electric sail motion, along with four corresponding Euler-Lagrange equations [20]. A total of eight suitable boundary conditions are, therefore, required to complete the mathematical problem, whereas a further scalar relationship is necessary to find the final time t_2.

Assume that the polar angle θ is measured from the apse line of the initial orbit. Then $\theta_0 \triangleq \theta(t_0)$ is the electric sail true anomaly at departure. The four initial boundary conditions are

$$\theta(t_0) = \theta_0, \qquad r(t_0) = \frac{a(1-e^2)}{1 + e\cos\theta_0}$$
$$u(t_0) = \frac{e\sin\theta_0}{\sqrt{a(1-e^2)/\mu_\odot}}, \qquad v(t_0) = \frac{1 + e\cos\theta_0}{\sqrt{a(1-e^2)/\mu_\odot}} \tag{3}$$

The remaining four boundary conditions at the final time t_2 depend on the particular mission typology and are discussed in the next section.

Mission Scenarios

Electric sail trajectories toward the SS boundaries are now investigated with different requirements and, correspondingly, different mission typologies.

Achievement of a Given Hyperbolic Excess Speed

In this first mission scenario, the sailcraft is required to reach a given hyperbolic excess speed $V_\infty \geq 0$ with respect to the SS in the least amount of time. The rationale for such a strategy is that V_∞ essentially coincides with the sailcraft cruise speed (that is, a uniform rectilinear motion [24]) in a hyperbolic trajectory toward the interstellar deep space. An early achievement of a substantial value of hyperbolic excess speed allows the spacecraft to jettison the electric sail. This simplifies the succeeding mission phases, thereby avoiding potential interferences with the payload instruments, and reduces the likelihood of a mission failure. Such a strategy has been proposed for similar deep space missions based on solar sails [4,25].

From a mathematical viewpoint, the problem amounts to prescribing the sailcraft mechanical energy $\mathcal{E}$ at the final instant t_2, that is

$$\mathcal{E}(t_2) \triangleq \frac{u(t_2)^2 + v(t_2)^2}{2} - \frac{\mu_\odot}{r(t_2)} = \frac{V_\infty^2}{2} \tag{4}$$

The three remaining boundary conditions necessary to obtain a stationary value of J involve the adjoint variables, viz, [26]

$$\lambda_\theta(t_2) = 0, \qquad \lambda_u(t_2) = \frac{\lambda_r(t_2)u(t_2)r(t_2)^2}{\mu_\odot}$$
$$\lambda_v(t_2) = \frac{\lambda_r(t_2)v(t_2)r(t_2)^2}{\mu_\odot} \tag{5}$$

The optimization problem is constituted by a two-point boundary value problem (2PBVP) for which the eight boundary conditions are given by Eqs. (3–5). The optimal final time t_2 is obtained by enforcing the transversality condition

$$H(t_2) = 1 \tag{6}$$

Note that the mission typology described in this section includes, as a particular case, the escape trajectories from the SS. In fact, the latter are obtained by setting the hyperbolic excess velocity equal to zero in Eq. (4), or, equivalently, $\mathcal{E}(t_2) = 0$.

Achievement of a Given Solar Distance

As a second mission scenario, consider the minimum-time trajectories to reach a given distance $r_2 > r(t_0)$ from the sun. These missions include both rapid flyby trajectories toward the outer planets and transfers toward the SS boundaries or the heliosheath [4,25,27]. The main difference with respect to the problem discussed in the preceding section is that now the parameter to minimize is the mission time necessary to reach r_2 irrespective of the value of V_∞. As a result, because the final hyperbolic excess speed is not explicitly used in the optimization process, in principle it is possible that the spacecraft cruise velocity at a distance r_2 be insufficient to continue the mission toward the deep space [27].

Using the final distance as the unique constraint on the probe trajectory (that is, both the spacecraft final angular position and its velocity components are left free), the following four boundary conditions are obtained at $t = t_2$:

$$r(t_2) = r_2, \qquad \lambda_\theta(t_2) \equiv \lambda_u(t_2) \equiv \lambda_v(t_2) = 0 \tag{7}$$

As in the preceding case, the flight time t_2 is found through Eq. (6), which, associated to Eqs. (3) and (7), completes the 2PBVP.

Constraints on Minimum Perihelion Distance

So far, no explicit constraint has been imposed on the minimum perihelion distance of the spacecraft trajectory. However, in both of the two preceding mission scenarios it is possible that, in an initial phase, the sailcraft goes toward the sun to exploit the increased available thrust resulting from the growing solar wind electron density and temperature [17,18,20]. Such a behavior, which will be referred to as solar wind assist (SWA), is similar (albeit based on a different physical mechanism) to the more familiar solar photonic assist concept [12,28,29] frequently used in solar sail based missions [4,25,27]. When a mission includes a SWA maneuver, it is necessary to guarantee that the sailcraft heliocentric distance does not fall below some $r_{\min} > 0$, that is, a minimum admissible value based on thermal and mechanical constraints involving the electric sail tethers. Preliminary estimates suggest assuming $r_{\min} = 0.5$ AU when aluminum tethers are used, whereas copper tethers are expected to guarantee a further reduction in the minimum distance up to $r_{\min} = 0.33$ AU[‡].

[‡](Janhunen, P., private communication, 2009)

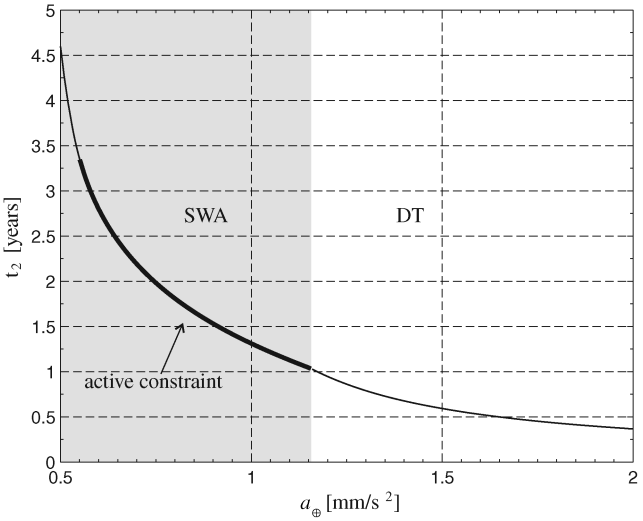

Fig. 2 Minimum escape times from Earth circular orbit (r_{min}= 0.5 AU).

From a mathematical point of view, the requirement on minimum perihelion distance can be taken into account with the addition of an inequality path constraint on the state variable r in the form [26]

$$r(t_1) \geq r_{min} \quad \text{for} \quad t_1 \in [t_0, t_2) \tag{8}$$

where t_1 is the time instant at which the minimum sun-sailcraft distance is reached. In practice, the optimal problem can be solved through a two step procedure. Firstly, a solution is found without imposing any path constraint. Let $r^\star$ be the minimum resulting distance from the sun. If $r^\star \geq r_{min}$, the corresponding trajectory is truly optimal and no further calculation is necessary. If, instead, $r^\star < r_{min}$ (thus implying that the constraint (8) would be violated), a second step is required. More precisely, a switching structure is assumed a priori [26], the constraint (8) (taken with the equality sign) is set active at $t = t_1$, and the sailcraft trajectory is divided into two arcs, corresponding to the approaching and departure phases, respectively. Invoking the transversality condition [26], the following two scalar relationships are found at the (unknown) time instant t_1

$$r(t_1) = r_{min}, \qquad u(t_1) = 0 \tag{9}$$

It may be shown that λ_r is the only adjoint variable discontinuous at t_1. In other terms, a three point boundary value problem (3PBVP) is now involved, in which both the time instant t_1 and the discontinuity (that is, the jump) in λ_r are found by imposing the two intermediate conditions (9). Note that the initial conditions (3), the final conditions (5) [or (7)] and the transversality condition (6), remain all unchanged.

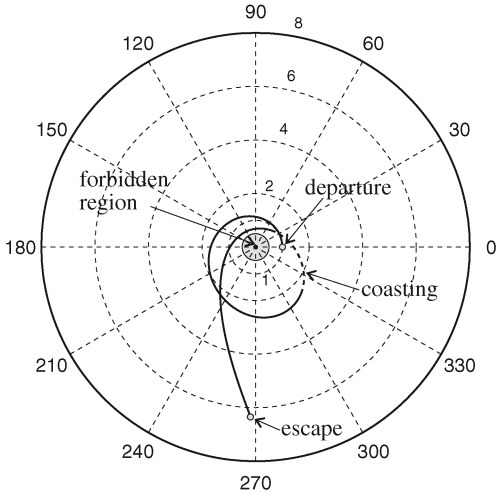

a) SWA with inactive constraint ($a_\oplus = 0.5\,\text{mm/s}^2$, $t_2 \simeq 4.6$ years).

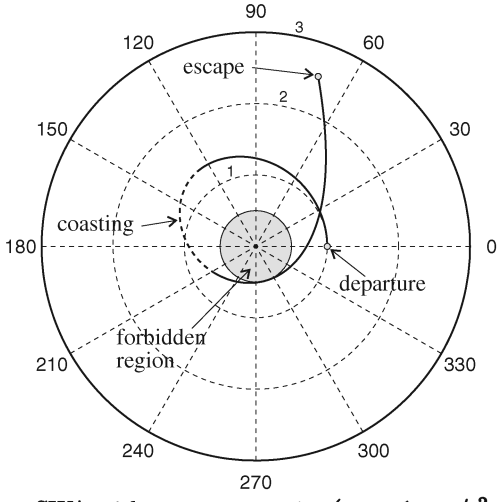

b) SWA with active constraint ($a_\oplus = 1\,\text{mm/s}^2$, $t_2 \simeq 1.31$ years).

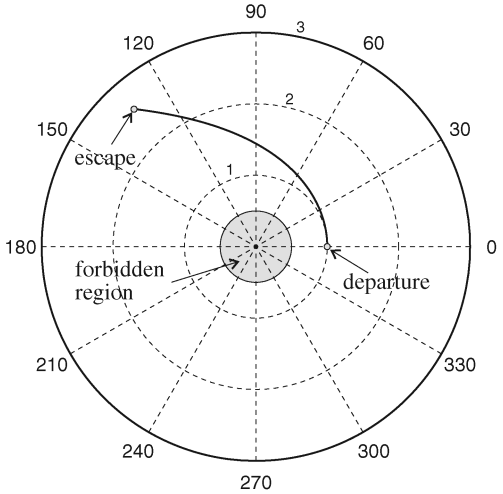

c) DT ($a_\oplus = 1.5\,\text{mm/s}^2$, $t_2 \simeq 0.59$ years).

Fig. 3 Escape trajectories from an Earth circular orbit (r_{min} = 0.5 AU).

Numerical Approach

The 2PBVP (or 3PBVP) associated to the variational problem has been solved through a hybrid numerical technique that combines genetic algorithms (to obtain an estimate of the initial adjoint variables) with gradient based and direct methods to refine the solution [10,30]. A set of canonical units [31] have been used in the integration of the differential equations to reduce their numerical sensitivity. The differential equations were integrated in double precision using a variable order Adams–Bashforth–Moulton solver [32,33] with absolute and relative errors of 10^{-12}. The final boundary constraints were set to 100 km for the position error and 0.05 m/s for the velocity error. These tolerance limits are sufficient for a preliminary mission analysis study.

Solar System Escape Trajectories

Consider first the problem of generating trajectories that allow an electric sail to escape from the SS using an Earth-escape parabolic trajectory, that is, with zero hyperbolic excess energy with respect to the planet (launch $C_3 \equiv 0$ km^2/s^2). This amounts to selecting $V_\infty = 0$ (or $\mathcal{E}(t_2) = 0$) in Eq. (4). The sensitivity of the minimum flight time t_2 to the sail performance has been studied in a parametric form by varying the sailcraft characteristic acceleration $a_\oplus$ in the range $[0.5, 2]$ mm/s^2. The upper limit corresponds to an estimated maximum value of the propelling acceleration at $r = r_\oplus$ that will probably be available in a near future. Two cases have been studied, corresponding to either a circular or an elliptical parking orbit. In both cases the maximum allowed cone angle is $\alpha_{\max} = 35$ deg, while the minimum perihelion distance is set to $r_{\min} = 0.5$ AU (aluminum tethers).

Escape from a Circular Orbit

In this first case, the starting orbit is circular with a radius equal to 1 AU. Accordingly, t_2 is independent of the sailcraft initial position (that is, of the launch date). This amounts to setting $\theta_0 = 0$, $e = 0$, and $a = 1$ AU in Eqs. (3). The mission times obtained from simulations are shown in Fig. 2 as a function of the characteristic acceleration.

The escape time is tolerable, being less than 4.6 years, even for moderate values of the characteristic acceleration. Note that as long as $a_\oplus$ is less than 0.55 mm/s^2 the optimal escape condition is reached without activating the constraint on $r_{\min}$. When the value of the characteristic acceleration ranges in the interval $[0.54, 1.16]$ mm/s^2, the spacecraft trajectory tends to approach the sun closer to exploit the thrust rise associated to the SWA. Accordingly, the constraint on the minimum admissible perihelion distance is activated. However, there exists a critical value of characteristic acceleration (equal to about 1.16 mm/s^2) over which the escape condition is more quickly obtained using a direct transfer (DT), that is, using a trajectory that increases, at any time, the instantaneous sailcraft distance from the sun. The spacecraft behavior is better understood with the aid of Fig. 3, which illustrates the sailcraft trajectory for three different values of characteristic acceleration. In particular, the three typologies correspond to a SWA trajectory with inactive constraint ($a_\oplus = 0.5$ mm/s^2), a SWA trajectory with active constraint ($a_\oplus = 1$ mm/s^2), and a DT trajectory ($a_\oplus = 1.5$ mm/s^2). Moreover, it may be shown by simulation that in a SWA strategy the minimum perihelion distance tends to continuously reduce as $a_\oplus$ is increased. A similar behavior was pointed out by Sauer [4] in his analysis of escape missions with solar sails.

Returning now to the three cases of Fig. 3, it is interesting to study the behavior of the specific mechanical energy $\mathcal{E}$ as a function of time, see Fig. 4. During a SWA trajectory there is a time interval characterized by $\dot{\mathcal{E}} < 0$ (a phase in which the sail thrust is used for approaching the sun) and a coasting phase ($\mathcal{E} =$ constant). On the contrary, in a DT trajectory the function $\dot{\mathcal{E}}$ is always positive and, therefore, $\tau \equiv 1$. In other terms the DT may be thought of as the globally optimal counterpart of a locally optimal strategy [34–38], in which the controls are chosen to maximize, at any time, the instantaneous variation of the mechanical energy $\dot{\mathcal{E}}$. The length of a coasting phase in a SWA trajectory is strongly dependent on the value

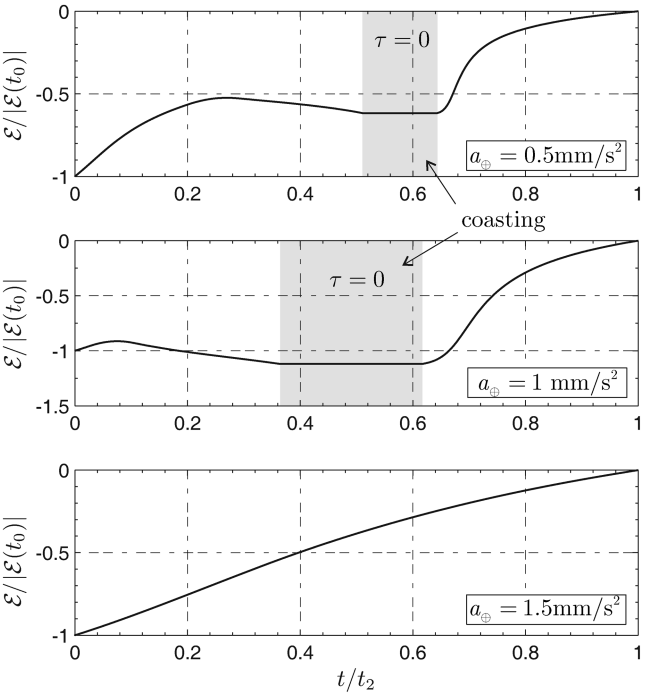

Fig. 4 Mechanical energy vs time for optimal escape trajectories from Earth circular orbit ($r_{\min} = 0.5$ mm/s^2).

of the characteristic acceleration. Figure 5 compares the sail cone angle $\alpha(t)$ for the three cases with $a_\oplus = (0.5, 1, 1.5$ mm/s$^2)$. While in a DT α is constant and equal to $\alpha_{\max} = 35$ deg during the whole mission, in a SWA trajectory, the cone angle experiences a sign variation during the perihelion approaching phase ($t \in [t_0, t_1]$). In terms of escape times, SWA and DT are equivalent strategies when $a_\oplus = 1.16$ mm/s^2 (in both cases $t_2 \simeq 1.03$ years). However, the corresponding escape distances $r(t_2)$ are much different, as illustrated in Fig. 6. The discontinuity in the crossing between the two strategies is better highlighted in Fig. 7, which shows the escape distance as a function of $a_\oplus$. The sensitivity of the escape time with respect to the value of $r_{\min}$ is shown Fig. 8. The flight times have been

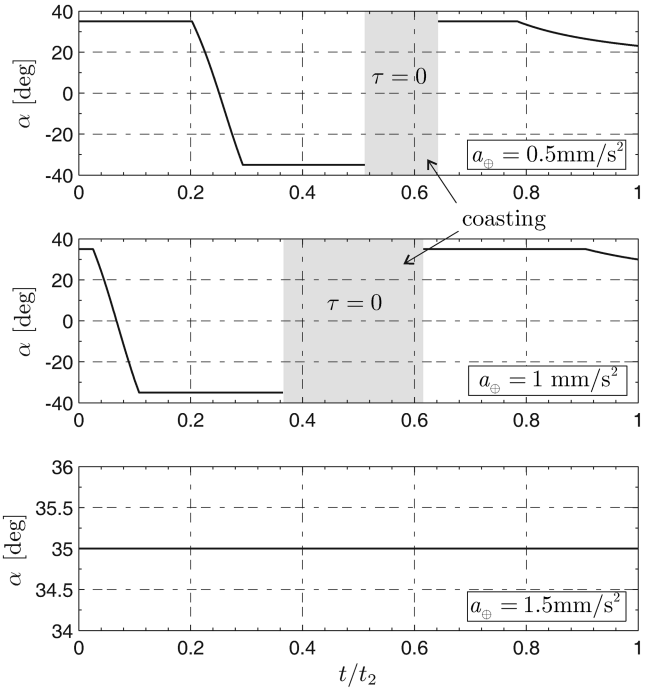

Fig. 5 Sail cone angle for minimum-time escape trajectories from Earth circular orbit ($r_{\min} = 0.5$ mm/s^2).

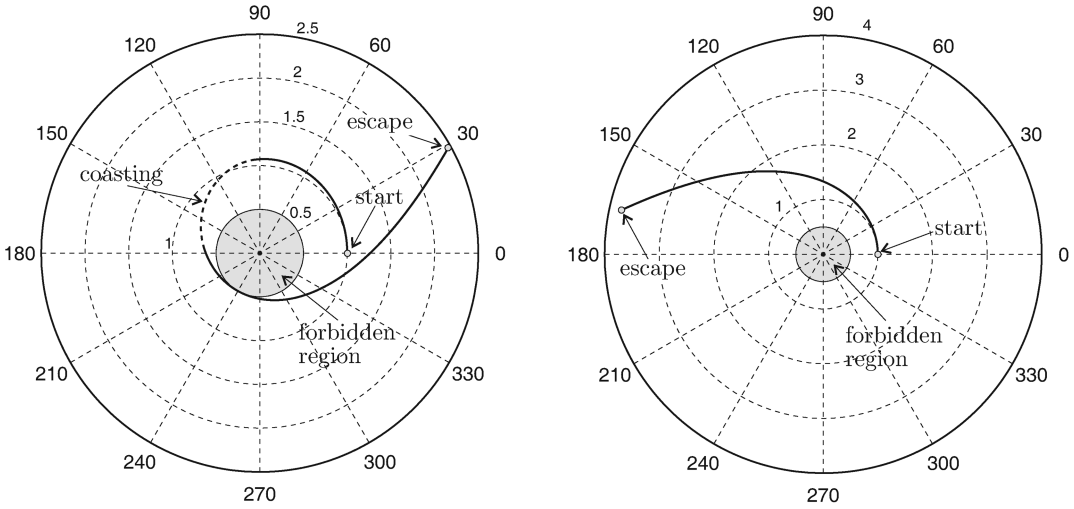

a) SWA b) DT

Fig. 6 Escape trajectory from Earth circular orbit for $a_\oplus = 1.16$ mm/s^2 ($t_2 \simeq 1.03$ years).

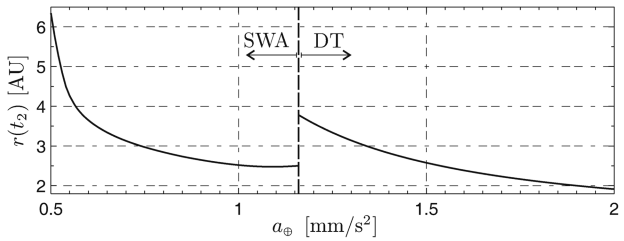

Fig. 7 Final distance for escape trajectories from Earth circular orbit as a function of $a_\oplus$ ($r_{\min} = 0.5$ AU).

normalized by the escape times corresponding to $r_{\min} = 0.5$ AU and taken from Fig. 2. The analysis is confined to the range $a_\oplus \in [0.55, 1]$ mm/s^2, within which from the preceding discussion $r(t_1) = 0.5$ AU. Figure 8 shows that the performance improvements obtained by decreasing $r_{\min}$ are moderate. For example, assuming $r_{\min} = 0.33$ AU (copper tethers), the reduction of escape time with respect to $r_{\min} = 0.5$ AU (aluminum tethers) is less than 8%.

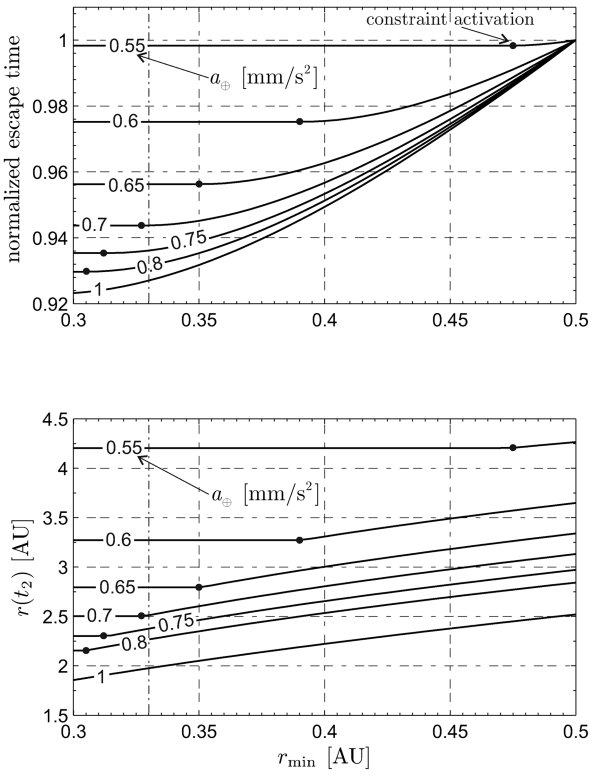

Fig. 8 Escape time from Earth circular orbit and final distance as a function of $a_\oplus$ and $r_{\min}$.

Escape from an Elliptic Orbit

In this case the initial orbit coincides with the real heliocentric orbit of Earth, that is, $a = 1$ AU and $e = 0.01671123$. Because the polar symmetry is lost, the mission performance must be studied by varying the initial true anomaly in the range $\theta_0 \in [0, 2\pi]$. It can be verified that the transition between SWA and DT strategies is essentially independent of θ_0 and is obtained when $a_\oplus \simeq 1.2$ mm/s^2. With reference to Fig. 9, the escape time t_2 is made dimensionless with its mean value $\bar{t}_2$ (calculated over θ_0), and the results have been separated according to the best escape strategy (either SWA or DT). The initial orbit eccentricity has a negligible effect on t_2 because the variation of $t_2/\bar{t}_2$ is always less than 5% when $a_\oplus$ ranges in the interval $[0.5, 2]$ mm/s^2. The optimal launch position in terms of θ_0 and the corresponding escape times have been summarized in Table 1. Note that the last table column shows the

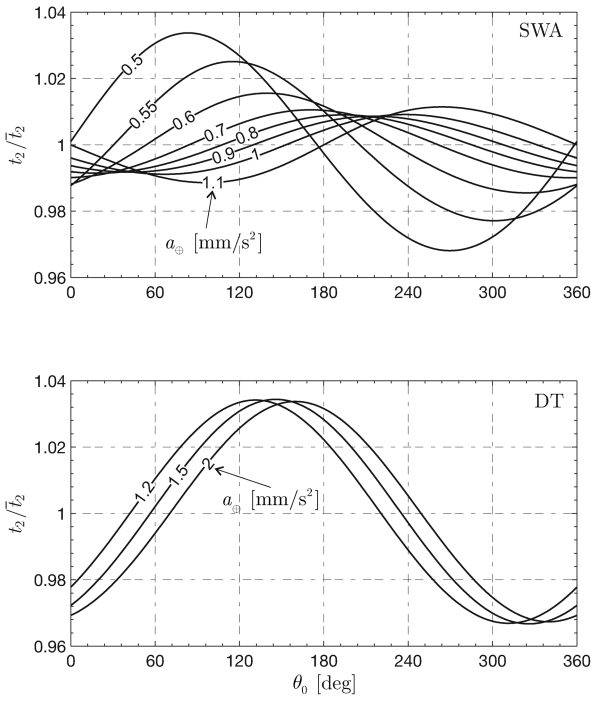

Fig. 9 Escape times from Earth elliptic orbit as a function of $a_\oplus$ and θ_0 ($r_{\min} = 0.5$ mm/s^2).

Table 1 Optimal conditions for escape from Earth elliptic orbit ($r_{min} = 0.5$ AU).

	Optimal Conditions							
$a_\oplus$, mm/s^2	t_2 ($e = 0$), yr	θ_0, deg	t_1, yr	$r(t_1)$, AU	$r(t_2)$, AU	$\theta(t_2)$, deg	t_2, yr	revolutions
0.5	4.599	270	2.993	0.6379	6.1499	174.38	4.449	1
0.6	2.802	324	2.094	0.5	3.6179	146.71	2.762	1
0.7	2.193	355	1.620	0.5	3.1205	136.55	2.172	1
0.8	1.811	19	1.305	0.5	2.8379	131.91	1.795	1
0.9	1.532	42	1.067	0.5	2.6476	130.8	1.519	1
1	1.314	67	0.8717	0.5	2.5281	132.89	1.302	1
1.1	1.131	96	0.6851	0.5	2.5064	136.68	1.118	1
1.2	0.946	311	0	0.9884	3.4933	113.21	0.9146	0
1.3	0.789	317	0	0.9873	3.0742	107.31	0.7629	0
1.4	0.676	322	0	0.9864	2.7623	102.92	0.6537	0
1.5	0.592	326	0	0.9858	2.5233	97.46	0.5719	0

number of electric sail revolutions around the sun before the escape condition attainment, whereas the second column summarizes the minimum escape times from a circular Earth orbit (see Fig. 2).

Two-Dimensional Trajectories Toward the Outer Solar System

In the preceding section the minimum time necessary to insert the electric sail into a parabolic orbit has been calculated. Once the escape condition is met, the propelling system may be jettisoned in such a way that the payload alone can continue its travel toward the deep space with a flight by inertia. Suppose now that the mission aim is to reach a given solar distance $r_2 \in [5, 100$ AU$]$ in the least amount of time. To avoid very long mission lengths, greater than 20 years when $r_2 = 100$ AU, electric sails with medium-high performance ($a_\oplus \in [1, 2]$ mm/s^2) will be considered. A preliminary analysis of this problem confirms that the Earth's orbital eccentricity has a negligible effect on the mission performance. Therefore, the initial parking orbit is assumed to be circular with a radius equal to 1 AU. The solutions of the optimal problem with boundary conditions given in Eq. (7) and a minimum perihelion distance $r_{min} = 0.5$ AU are summarized in Fig. 10.

The DT strategy is superior to the SWA in the gray region highlighted in Fig. 10. This region is confined to somewhat small values of r_2 when compared with the characteristic dimensions of the SS and to the heliosheath distance (roughly 100 AU). For example, assuming the maximum admissible value of characteristic acceleration, that is, $a_\oplus = 2$ mm/s^2, a DT is superior to a SWA transfer provided that $r_2 < 13$ AU. In particular, Fig. 10 shows that for medium-high performance electric sails (with $a_\oplus \in [1, 2]$ mm/s^2) a rapid flyby trajectory toward Jupiter (or to the asteroid belt) favors a DT. When rapid flybys toward Saturn are concerned, a SWA strategy is preferable for electric sails with characteristic accelerations less than 1.1 mm/s^2. Finally, missions toward the outer SS require a SWA strategy unless very high performance electric sails are considered (that is, $a_\oplus > 4$ mm/s^2).

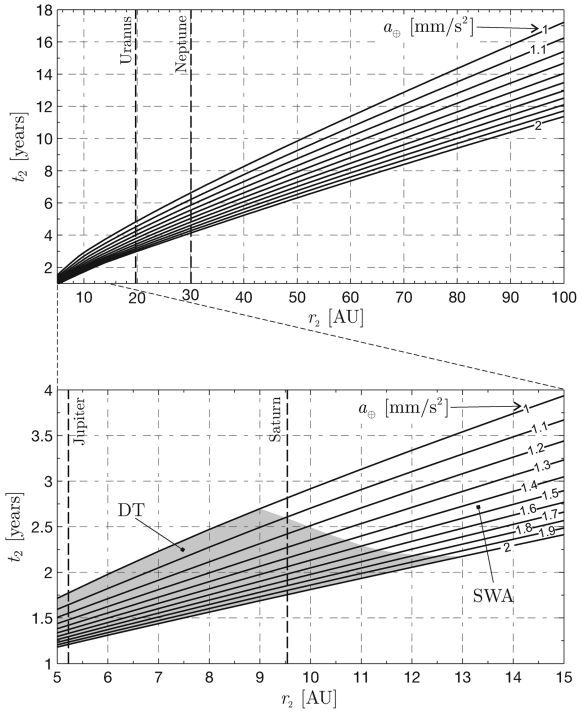

Fig. 10 Minimum flight time t_2 vs final solar distance r_2 (r_{min}= 0.5 AU).

The simulations show that in all of the analyzed cases the specific mechanical energy at r_2 is positive. This means that the sailcraft at the end of its nominal trajectory is on a hyperbolic orbit that eventually leaves the SS. This point is highlighted in Fig. 11, which also shows the value of V_∞ at the final time t_2. Recall, however, that the hyperbolic excess speed shown in Fig. 11 is not the maximum attainable value at $r = r_2$, rather it is the value that the sailcraft obtains at the end of the minimum-time trajectory necessary to reach the desired distance r_2. Note that V_∞ takes high values especially when substantial characteristic accelerations are used. For example, assuming $a = 2$ mm/s^2, one has $V_\infty \simeq 10$ AU/year at the end of a mission toward the heliosheath ($r_2 \simeq 100$ AU). This hyperbolic excess speed is sufficiently high to allow the sailcraft to extend the original mission and continue its travel with a cruise speed roughly coincident with V_∞. To make a comparison with current missions, Voyager 1 is escaping from the SS at a speed of about 3.6 AU/year, while Voyager 2 is escaping at a speed of 3.3 AU/year.[§] Fig. 11 shows a discontinuity in the contour line caused by the strategy variation. Note, however, that this discontinuity is missing in Fig. 10 because the transition between DT and SWA is here controlled by the total mission time and not by the value of V_∞.

The possibility of a mission extension is a particularly important feature for trajectories toward the outer SS space, in which a certain distance must be obtained in a given time and with a prescribed value of hyperbolic excess speed [25]. From this point of view the simulations have shown that the perihelion constraint (in the range $r_{min} \in [0.3, 0.5]$ AU) does not significantly affect the mission performance. This is clear from Fig. 12 in which the flight time t_2 and the hyperbolic excess speed V_∞ are shown as a function of the characteristic acceleration and r_{min} for minimum-time missions toward heliosheath ($r_2 = 100$ AU).

In particular, assuming $r_{min} = 0.5$ AU, the flight time can be approximated with an error less than 10 days through the following simplified relationship

$$t_2 \approx \frac{17.18}{a_\oplus^{0.6}} \tag{10}$$

in which t_2 is expressed in years, and $a_\oplus$ in millimeters per square second. Equation (10) gives a semi-analytic, first-order relationship between the time necessary to reach the heliosheath and the electric sail performance in terms of characteristic acceleration. Such a

[§]Data available from http://voyager.jpl.nasa.gov/mission/interstellar.html [retrieved 14 Oct. 2009]

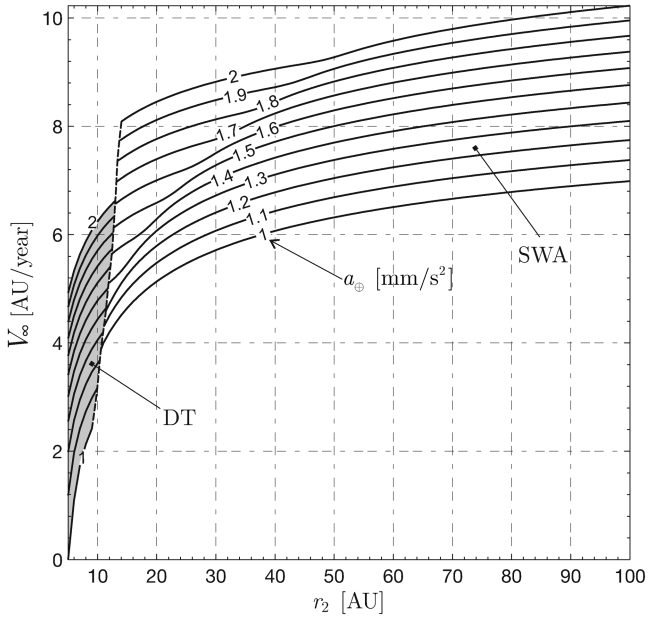

Fig. 11 Hyperbolic excess speed V_∞ as a function of the final solar distance r_2 ($r_{\min} = 0.5$ AU).

relationship will be the starting point for a second order analysis, discussed in the next section, which takes into account the actual 3-D of the problem at hand.

Figure 12, or Eq. (10) if $r_{\min} = 0.5$ AU is assumed, shows that the heliosheath may be reached in about 15 years with a medium-performance electric sail, having a characteristic acceleration of 1.15–1.25 mm/s^2. As a comparative example, Voyager 1 has reached a solar distance of 100 AU in 2006, that is, 29 years after its departure.

In analogy to the escape trajectories from the SS, missions toward the heliosheath are characterized by the constraint activation on the minimum distance from the sun and by a single coasting phase. This behavior is illustrated in Fig. 13 which shows the trajectory toward $r_2 = 100$ AU with $a_\oplus = 1$ mm/s^2 along with the time history of the

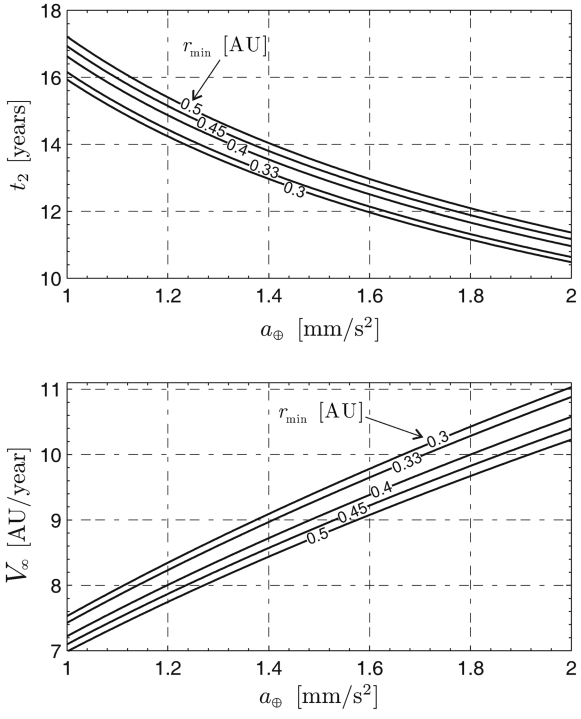

Fig. 12 Optimal performance for missions toward the heliosheath ($r_2 = 100$ AU).

cone angle α. Figure 13b shows that the coasting phase, for which the time length is 1.4 years, starts about 10 months after the departure. The escape condition ($\mathcal{E} = 0$) is obtained after 2.4 years from the launch.

Near-Minimum-Time Trajectories

So far, the electric sail has been employed during the whole trajectory length, with the only exception of the coasting phases. With the aid of Fig. 12, one concludes, for example, that the propelling system would be engaged for about 17 years if $a_\oplus = 1$ mm/s^2 or 11 years if $a_\oplus = 2$ mm/s^2 when $r_{\min} = 0.5$ AU. These high values of time intervals suggest to investigate different (that is, not optimal) strategies to reach the heliosheath. An interesting alternative is obtained by observing that when SWA strategies are employed to approach the outer SS, the sailcraft covers a nearly rectilinear trajectory when r is greater than about 15 AU, see Fig. 13a. Therefore, the spacecraft motion experiences an accelerated motion with a very low acceleration value for which the modulus tends progressively to decrease as the sailcraft moves away from the sun. Assuming that the propulsion system is switched off during this nearly rectilinear trajectory phase, one would obtain a slightly decelerated motion with a terminal velocity equal to the value of V_∞ attained when the thrust is set to zero. Actually, the simulations show that if one switches off the thrust at any point during the nearly rectilinear trajectory phase, the sailcraft velocity is essentially equal to the hyperbolic excess speed corresponding to the osculating orbit calculated at the switching-off instant, see Fig. 14. Therefore, an alternative and near-minimum-time strategy to reach high SS distances in a 2-D framework could be that of maximizing V_∞ for a given flight time (the latter value might be chosen by taking into account the propulsion system requirements and the mission constraints).

With such a strategy, the thrust may be switched off at t_2 and the sail may be jettisoned. Note that the problem of maximizing V_∞ for a given t_2 is nearly equivalent to that of minimizing the flight time necessary to reach a given hyperbolic excess speed with respect to the SS. Therefore, it is possible to use the mathematical model with boundary constraints discussed earlier (5). The following analysis is confined to thrust-on times less than 10 years [39] and is characterized by moderate values of $a_\oplus$ in the range [0.6, 1] mm/s^2. The simulation results are summarized in Fig. 15. For example, a characteristic acceleration $a_\oplus = 1$ mm/s^2 allows one to obtain a hyperbolic excess speed of about 7 AU/year at $r(t_2) \simeq 33$ AU when $t_2 = 10$ years. Assuming that at $t = t_2$ the motion is rectilinear uniform with a velocity $V \triangleq \sqrt{u(t_2)^2 + v(t_2)^2}$ equal to V_∞ (see Fig. 14), the sailcraft would require $(100 - 33)/7 \simeq 9.6$ years to reach the heliosheath distance $r_2 = 100$ AU, and the total mission time would be $(10 + 9.6) = 19.6$ years. As a comparison with an optimal trajectory, Fig. 12 shows that, using $r_{\min} = 0.5$ AU and $a_\oplus = 1$ mm/s^2, the minimum flight time is about 17.2 years. If, instead, one maximizes the hyperbolic excess velocity, the additional time necessary to reach the heliosheath distance is 2.4 years, with an increase of +14% with respect to the minimum admissible value. However, the corresponding propulsion system engagement decreases dramatically from 17.2 years (in the minimum-time case) to 10 years (in the maximum V_∞ case), with a percentage reduction of 42%.

When a near-minimum-time strategy is used, the electric sail performance is strongly influenced by the minimum admissible value of perihelion radius. In fact, the sailcraft tends to approach, as much as possible, the sun to fully exploit the SWA effect and to maximize the hyperbolic excess velocity. This behavior is better appreciated with the aid of Fig. 16, in which the influence of $r_{\min}$ on the flight time is shown for different values of the hyperbolic excess speed when $a_\oplus = 1$ mm/s^2. Note that the mission times are made dimensionless with the values corresponding to $r_{\min} = 0.5$ AU (the latter may be taken from Fig. 15).

Using the data from Fig. 16, if one uses $r_{\min} = 0.33$ AU (copper tethers), a sailcraft hyperbolic excess velocity of $V_\infty = 7$ AU/year is reached within a time length equal to 63% the time necessary to obtain the same V_∞ with $r_{\min} = 0.5$ AU (aluminum tethers).

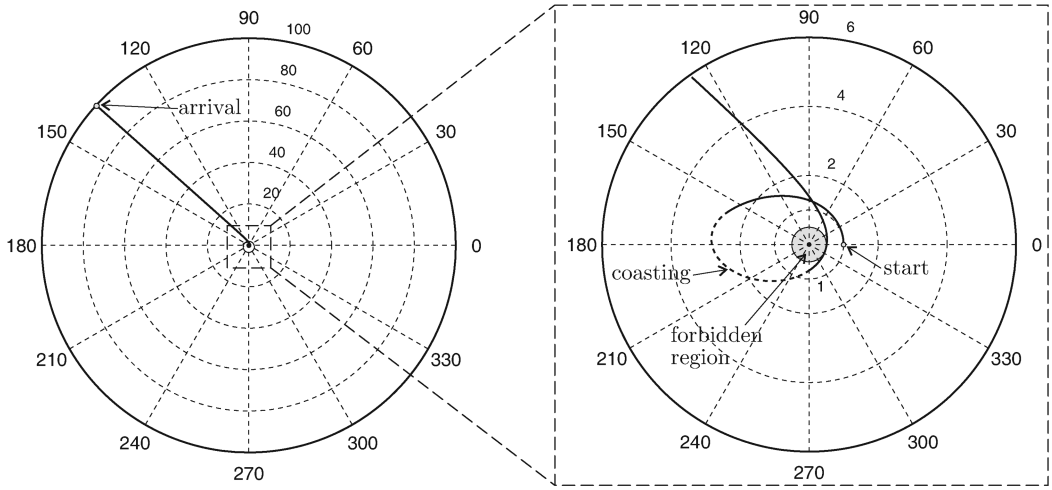

a) Optimal trajectory

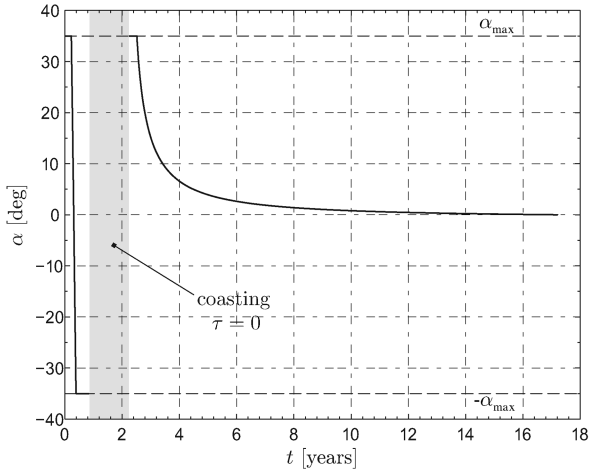

b) Sail cone angle vs. time

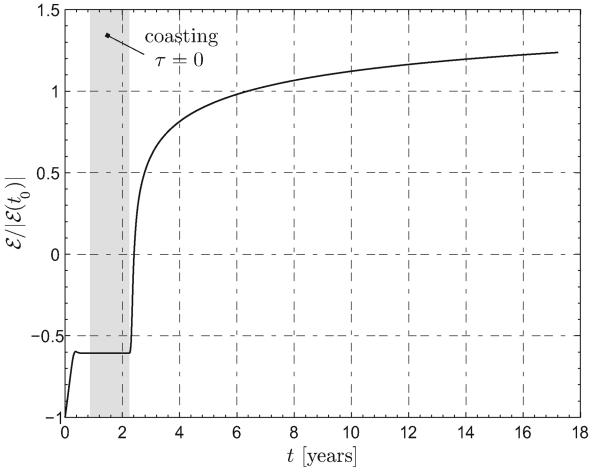

c) Mechanical energy vs. time

Fig. 13 Minimum-time trajectory toward the heliosheath ($r_2 = 100$ AU) for $a_\oplus = 1$ mm/s^2 and $r_{min} = 0.5$ AU.

Because a hyperbolic excess of 7 AU/year requires 10 years when $a_\oplus = 1$ mm/s^2 and $r_{min} = 0.5$ AU (see Fig. 15) a closer approach to the sun, up to 0.33 AU, guarantees a mission time decrease of about 3.7 years. Similar conclusions can be obtained in terms of final solar distance $r(t_2)$.

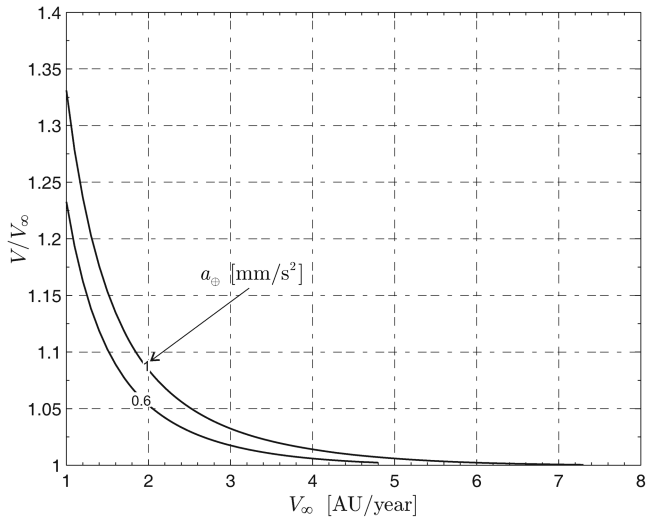

Fig. 14 Final sailcraft speed as a function of V_∞ and $a_\oplus$ (r_{min}= 0.5 AU).

Three-Dimensional Trajectories Toward the Heliosheath

The preceding analysis, under the simplified assumption of a 2-D problem, provides a first-order estimate of the minimum performance (in terms of characteristic acceleration) required by the electric sail to either attain a flyby with an outer planet or to reach the boundaries of the SS (that is, distances on the order of 100 AU) in a given time interval t_2. In this section transfers toward the heliosheath and the heliopause will be studied by taking into account the 3-D of the actual electric sail trajectory. In fact, both the heliosphere and the heliosheath are shaped by the interaction of the solar wind with the local interstellar medium, as the Earth's magnetosphere is made droplet shaped by the solar wind [7]. Currently, the ecliptic latitude and longitude of the heliosheath nose are given by $\phi_H = 7.5$ deg and $\psi_H = 254.5$ deg, respectively.

Because the sailcraft longitude at the final instant t_2 is strictly connected to its initial position on the departure orbit, the earlier estimated mission times are certainly less than that achievable with a truly 3-D trajectory. To quantify such differences the mathematical problem must be slightly changed with the introduction of a suitable inertial spherical reference system $\mathcal{T}_\odot(r, \psi, \phi)$, where ψ is the ecliptic longitude and ϕ is the ecliptic latitude. The corresponding electric sail equations of motion and the Euler–Lagrange equations are here omitted for the sake of conciseness. The interested reader is referred to [22] for a detailed discussion of those equations along with the optimal control law involving the three control variables τ, α, and δ. The clock angle δ points out the propelling thrust angle in the plane perpendicular to the sun-sailcraft direction.

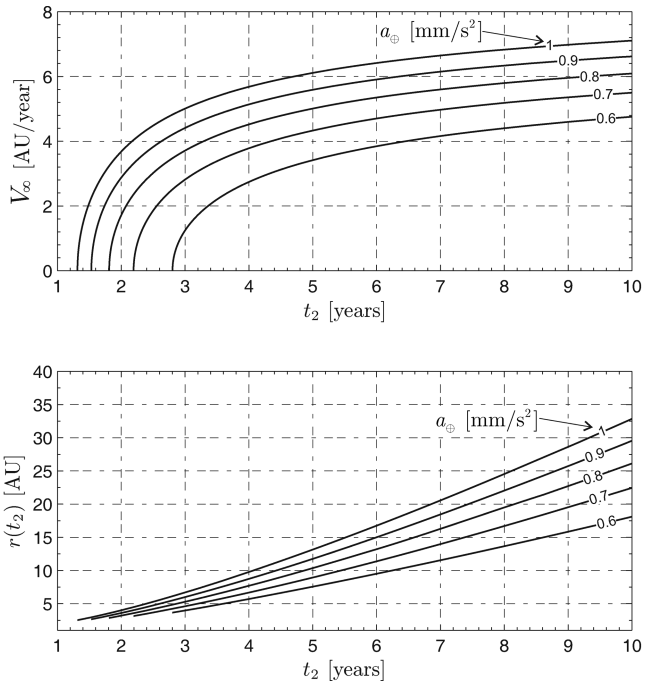

Fig. 15 Minimum time to reach a given V_∞ ($r_{\min} = 0.5$ AU).

Contrary to the planar case, in a 3-D space the cylindrical symmetry of the problem is lost. This happens even for a circular initial orbit (recall that the Earth's orbital eccentricity has a negligible effect on the mission time) because of the existence of a preferential direction in the space. The latter coincides with the line joining the sun with the heliopause nose and is characterized through ψ_H. In mathematical terms, the starting sailcraft longitude $\psi_0 \triangleq \psi(t_0)$ is an unknown of the problem, for which the value may be found by imposing the final condition $\psi(t_2) = \psi_H$. The total mission time t_2 is found by enforcing the transversality condition (6), whereas the initial value of λ_ϕ is obtained through the condition $\phi(t_2) = \phi_H$ at the final time.

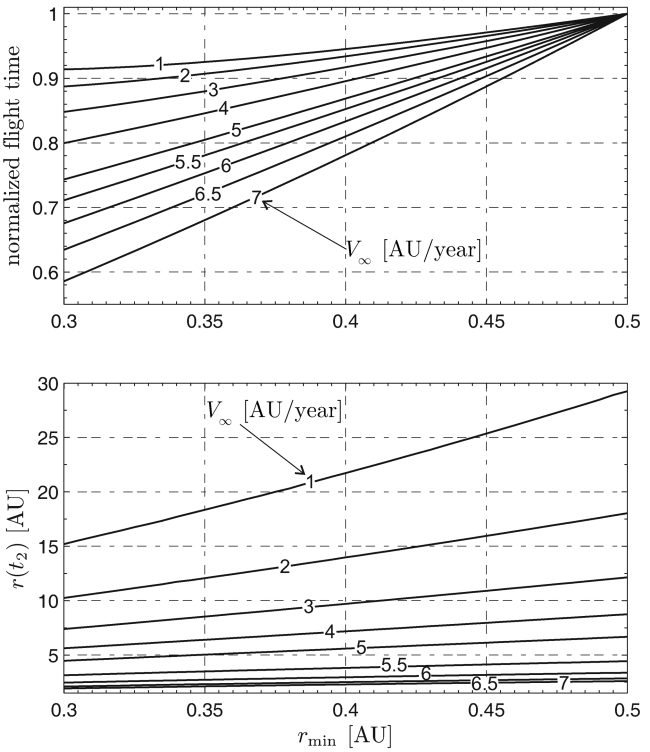

Fig. 16 Flight time and final solar distance as a function of $r_{\min}$ and V_∞ when $a_\oplus = 1$ mm/s^2.

Minimum-time trajectories toward the heliosheath nose have been studied assuming an initial circular orbit with radius equal to 1 AU and a minimum distance $r_{\min} = 0.5$ AU. From the earlier 2-D analysis, the characteristic acceleration ranges in the interval $a_\oplus \in [1, 2]$ mm/s^2, the propelling thrust is assumed to be available for the whole mission time, and the constraint on the minimum distance is set active. The variation of t_2 with $a_\oplus$ is illustrated in Fig. 17a, in which the flight time corresponding to the 2-D case is displayed for comparison (see also Fig. 12).

Figure 17a shows the increase of t_2 in the transition from the 2-D to the 3-D case. Such an increase varies between 5 and 15% for electric sails with medium-high performance ($a_\oplus \in [1.2, 1.8]$ mm/s^2) and tends to reduce with an increase of the characteristic acceleration. For example, when $a_\oplus = 2$ mm/s^2 the difference in flight time for the 2-D models is only 5 months, that is less than 3.5% of the total mission time. Figure 17a also shows that the 2-D analysis is unsuitable for characteristic accelerations approximately (or less than) $a_\oplus = 1$ mm/s^2 when the differences exceed 26%. Such a behavior may be explained by observing that the required variation of the orbital plane takes place during the approaching phase to the sun and soon after the SWA, when the propelling acceleration attains its maximum value. Unlike the 2-D case, the propelling acceleration is used, in part, to vary the value of ϕ instead of increasing the sailcraft specific mechanical energy. This reduced capability of exploiting the SWA in a 3-D trajectory increases with a decrease of $a_\oplus$ and is ultimately

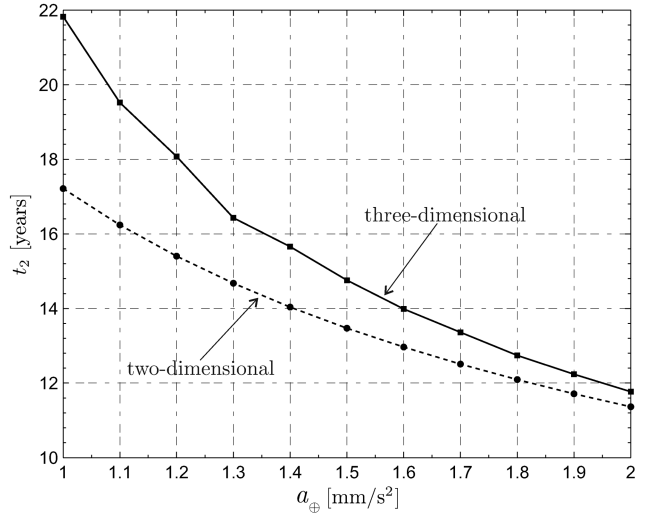

a) Flight time

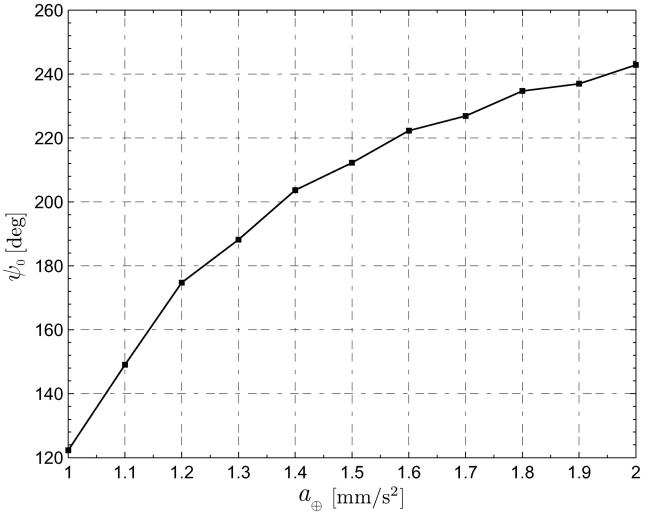

b) Initial heliocentric longitude

Fig. 17 Mission performance toward the heliosheath nose (r_2= 100 AU) with $r_{\min} = 0.5$ AU.

responsible for the growing differences in mission times between the two models.

Figure 17b shows the variation in initial sailcraft longitude ψ_0 with $a_\oplus$. The information on the value of ψ_0 allows one to estimate the sailcraft launch window. Because the position of the heliosheath nose is nearly independent of time, the launch window obtainable from Fig. 17b repeats every year.

As outlined in the 2-D analysis, the use of an electric sail for the whole mission time implies that the propulsion system must operate for a time length of 10–20 years, depending on the value of $a_\oplus$. Because the modulus of the propelling acceleration decreases sharply with the sun's distance (for example $a_p/a_\oplus \simeq 6.8\%$ when $r = 10$ AU), it is possible to imagine a mission strategy in which the sail is jettisoned at a distance r_c. Such a strategy, similar to what was studied by Sauer [4] for solar sails, plans a flight by inertia between r_c and r_2, thus simplifying the acquisition of science data without any interference with the sail. Using such a mission strategy, several new trajectories toward the heliosheath nose have been simulated. In accordance with Sauer [4], and to obtain a direct comparison with solar sails, a cutoff distance of $r_c = 5$ AU was enforced in the simulations. Also, only solutions with flight times less than 20 years have been considered. The simulation results, using three possible values of minimum solar distance $r_{\min} = (0.33, 0.4, 0.5)$ AU, are summarized in Fig. 18. A mission toward the heliosheath with $r_c = 5$ AU and a flight time less than 20 years requires, in the most favorable case ($r_{\min} = 0.33$ AU), a characteristic acceleration of at least 1.35 mm/s^2. Moreover, using the results from Sauer [4] for comparative purposes, one observes that, the minimum perihelion distance being equal ($r_{\min} = 0.4$), the electric sail and the solar sail present similar performance for $a_\oplus \simeq 2$ mm/s^2, whereas for smaller values of characteristic acceleration a solar sail is definitely superior to an electric sail. The reason is that a solar sail has a more pronounced thrust increase with respect to an electric sail in the nearness of the perihelion (recall that for a solar sail, the thrust varies as $1/r^2$). On the other hand an electric sail produces a higher thrust for distances $r > r_\oplus$, but such an advantage is reduced by the constraint on r_c.

It is interesting to investigate the influence of r_c on the mission time t_2. Assuming $r_{\min} = 0.5$ AU and varying the cutoff distance in the range $r_c \in [5, 30]$ AU, which corresponds to jettison the sail at a sun's distance between Jupiter and Neptune, one obtains the results shown in Fig. 19. When the sail is jettisoned at a distance greater than 15 AU, it is possible to reach the heliosheath nose in less than 20 years using characteristic accelerations that do not exceed 1.3 mm/s^2. Of course, it must be guaranteed that this mission scenario does not breach the continuous science data acquisition requirement. Alternatively, if one uses a sufficiently high characteristic acceleration, say $a_\oplus = 1.5$ mm/s^2, and assuming

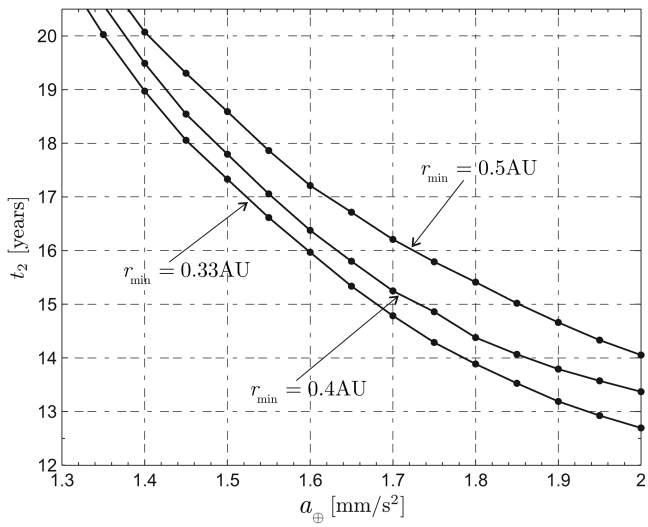

Fig. 18 Flight time for missions toward heliosheath nose ($r_2 = 100$ AU) with $r_c = 5$ AU.

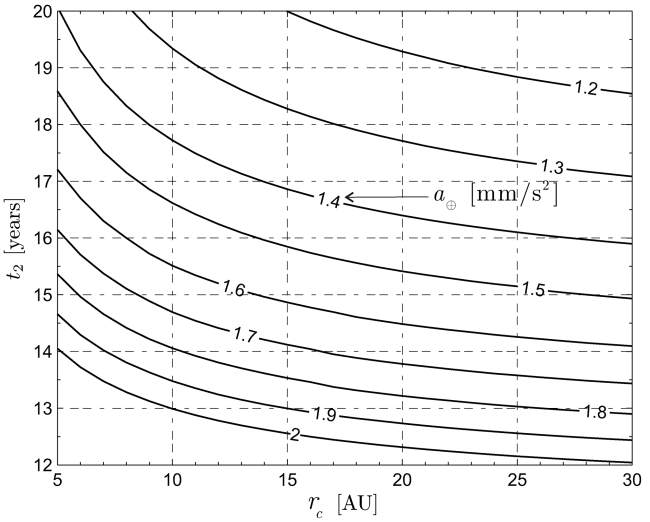

Fig. 19 Flight time for missions toward heliosheath nose ($r_2 = 100$ AU) as a function of r_c with $r_{\min} = 0.5$ AU.

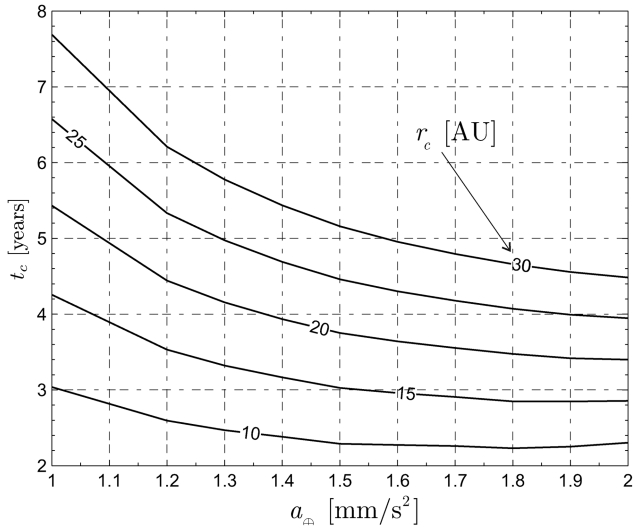

Fig. 20 Sailing mode time t_c as a function of r_c and $a_\oplus$ ($r_{\min} = 0.5$ AU).

$r_c = 15$ AU, one obtains a timesaving of more than 2.5 years with respect to the case in which the sail is jettisoned at a distance of 5 AU from the sun. Clearly, as r_c is increased, the sail operating time length $t_c \triangleq t(r = r_c)$ increases as well, as is shown in Fig. 20. Such a time length will now be referred to as sailing mode time. Note that t_c does not, in general, coincide with the time length t_{on} in which the sail produces a thrust ($\tau = 1$), because the optimal trajectory may include the presence of coasting arcs. In other terms $t_c \geq t_{\text{on}}$, and the equality sign takes place only provided that the trajectory displays no coasting arcs. Therefore, from Fig. 20 one deduces that if $r_c < 30$ AU and $a_\oplus > 1.2$ mm/s^2 the time t_{on} is less than 6 years, that is, is much less than the propulsion system lifetime of 10 years conjectured in [39]. The hyperbolic excess speed V_∞ varies, in its turn, with r_c, as is shown in Fig. 21, and is less than 10 AU/years in all of the simulations. The value of V_∞ is a particularly important datum if one considers a possible extension for a mission originally planned to reach the heliosheath nose. This matter is further discussed in the next section.

Electric Sail as a Propulsion Option for the Interstellar Heliopause Probe

From the earlier analysis, it is apparent that an electric sail with a characteristic acceleration of about 2 mm/s^2 may represent an interesting alternative to the conventional propulsion systems and to

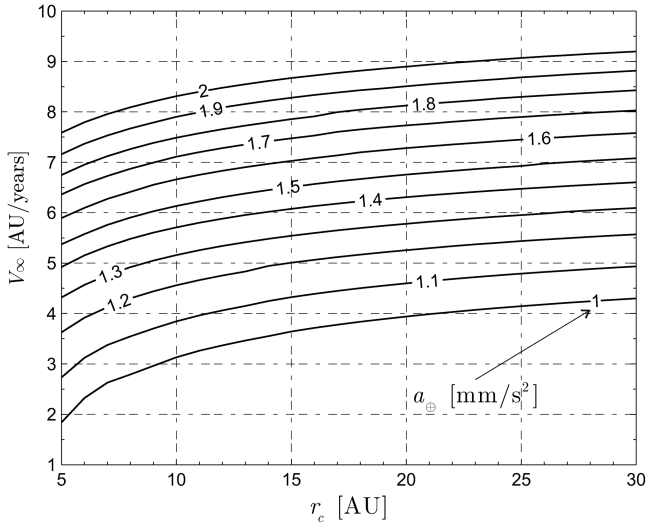

Fig. 21 Hyperbolic excess speed as a function of r_c and $a_\oplus$ ($r_{\min}$= 0.5 AU).

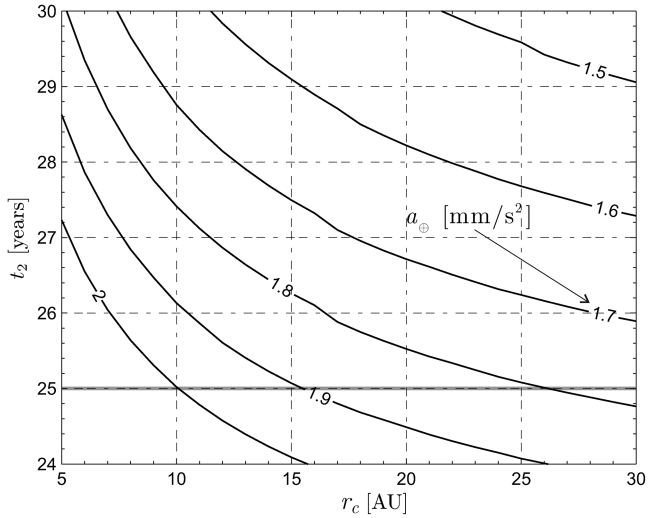

Fig. 22 Approximated flight time for missions toward the heliopause nose ($r_2 = 200$ AU) with $r_{\min} = 0.5$ AU.

the solar sails for a mission toward the boundaries of the SS. In particular, it is now interesting to investigate whether an electric sail may be considered as a potential primary propulsion system for a particular mission, such as the Interstellar Heliopause Probe (IHP) [7,28,40]. This mission is one of the four technology reference studies [6] introduced by the Planetary Exploration Studies Section of the Science Payload and Advanced Concept Office at ESA.

The IHP primary scientific aim [7] is that of analyzing the heliopause and the interstellar medium through in situ measurements with a highly miniaturized and a highly integrated payload suite [6]. Preliminary studies [7,40] have estimated that the payload suite, with a mass of about 20 kg, can be accommodated inside a small spacecraft (the spacecraft platform) having an overall mass of $m_p = 213$ kg. Such a platform, equipped with a suitable propulsion system, should be able to reach the heliopause ($r_2 = 200$ AU) within 25 years of transfer time [40]. Three primary propulsion systems have been examined so far, chemical propulsion, nuclear electric propulsion, and solar sailing. A solar sail was the only solution capable of meeting all the mission requirements [6], especially as far as the total mission time is concerned. In addition, the current conception of IHP mission requires that the primary propulsion system (that is, the solar sail) is jettisoned at a solar distance of 5 AU. As discussed above, this choice simplifies the scientific measurements avoiding any interference with the sail and, at the same time, reduces the propulsion system operating time, thus reducing the mission failure probability [4].

Before analyzing such a mission toward the heliopause nose in an optimal framework, the earlier simulations are used to obtain an approximate estimate of the required electric sail performance. To this end, under the assumption of Keplerian motion (this is the case if the sail is jettisoned at a distance r_c from the sun) the sailcraft attains its cruise phase with a uniform rectilinear motion at a distance $r \simeq 100$ AU and with a velocity equal to V_∞. Let t_{100} be the time length necessary to reach the heliosheath nose (see Fig. 19). Observing that the further distance required by the sailcraft to pass from the heliosheath to the outer boundary of heliosphere is about $\Delta r = 100$ AU, the minimum required flight time can be approximated as

$$t_2 \simeq t_{100} + \frac{\Delta r}{V_\infty} \tag{11}$$

Because t_{100} and V_∞ are both functions of $a_\oplus$ and r_c (see Figs. 19 and 21), and assuming $r_{\min} = 0.5$ AU, the flight time t_2 can be expressed in graphical form as shown in Fig. 22. A slightly reduced value of t_2 could be obtained by decreasing the constraint on $r_{\min}$. From Fig. 22 and Eq. (11) one concludes that a mission toward the heliopause, with the constraint of not exceeding 25 years of flight time and with a sail jettison at a distance less than 30 AU, would require an electric sail with a characteristic acceleration not less than 1.8 mm/s^2. Also, unlike the solar sail option [7,40], an electric sail jettison at a distance of 5 AU is unfeasible unless one tolerates much higher values of characteristic acceleration. In practice, from Fig. 22, the minimum tolerable distance at which an electric sail could be jettisoned is about 10 AU, a distance comparable to that of Saturn.

Using three reasonable values of characteristic acceleration, that is, $a_\oplus = (1.8, 1.9, 2)$ mm/s^2, and estimating the jettison distance r_c from Fig. 22, the minimum-time trajectory toward the heliopause ($r_2 = 200$ AU, $\psi(t_2) = \psi_H$, and $\phi(t_2) = \phi_H$) has been found by solving an optimal control problem as discussed earlier. The results corresponding to the three simulations have been summarized in Table 2. All of the three cases give the same launch window (ecliptic longitude $\psi_0 \simeq 190$ deg) and provide nearly the same value of hyperbolic excess speed $V_\infty \simeq 8.3$ AU/year. This result agrees with the data shown in Fig. 21. From Table 2, the time t_{on} during which the electric sail operates is, in the worst case with $a_\oplus = 1.8$ mm/s^2, slightly superior to 3.5 years. By comparing the value of t_{on} with that of t_c (the latter being taken from Fig. 20), one deduces that in the interval $t \in [t_0, t_c]$ the optimal trajectory displays at least one coasting phase. A more detailed analysis has revealed that in all of the simulation cases such a coasting phase is actually unique and stops shortly before the reaching of the perihelion at a distance of 0.5 AU from the sun. The coasting phase and the time history of the state variables are shown in Fig. 23, which illustrates the simulation results corresponding to $a_\oplus = 2$ mm/s^2. For the sake of clearness, the time scale is confined to 2.5 years from the departure. From Fig. 23, as discussed earlier, the change of latitude takes place in the first trajectory phase and the escape conditions are met after 1.2 years from the departure. The 3-D trajectory and its projection on the ecliptic plane are shown in Fig. 24. The time history of the three

Table 2 Mission toward the heliopause nose ($r_2 = 200$ AU) with $r_{\min} = 0.5$ AU.

$a_\oplus$, mm/s^2	r_c, AU	ψ_0, deg	t_1, yr	t_c, yr	t_2, yr	t_{on}, yr	V_∞, AU/yr
1.8	26	189.4	0.935	4.19	24.99	3.69	8.31
1.9	15	190	1.034	2.87	24.97	2.28	8.32
2.0	10	190.2	1.157	2.34	24.9	1.66	8.36

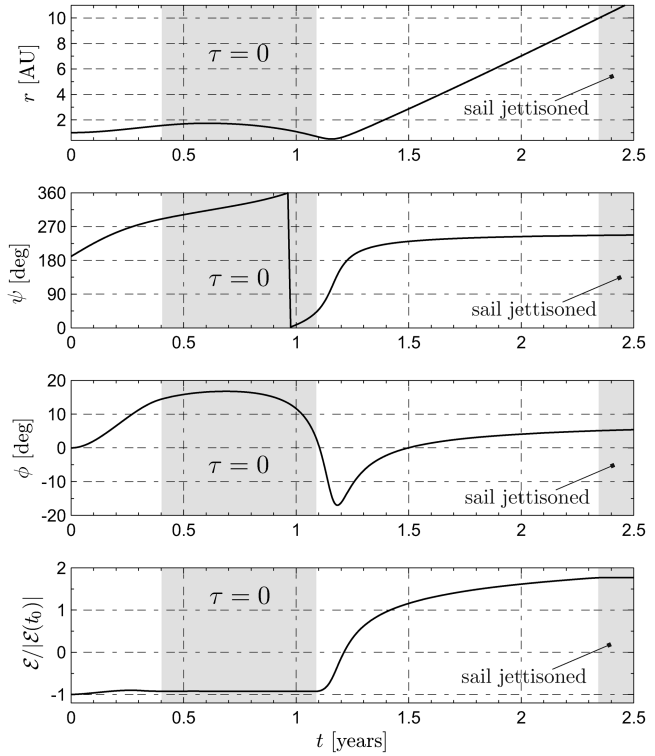

Fig. 23 State parameters time histories for a mission toward the heliopause nose ($r_{\min} = 0.5$ AU and $a_\oplus = 2$ mm/s^2).

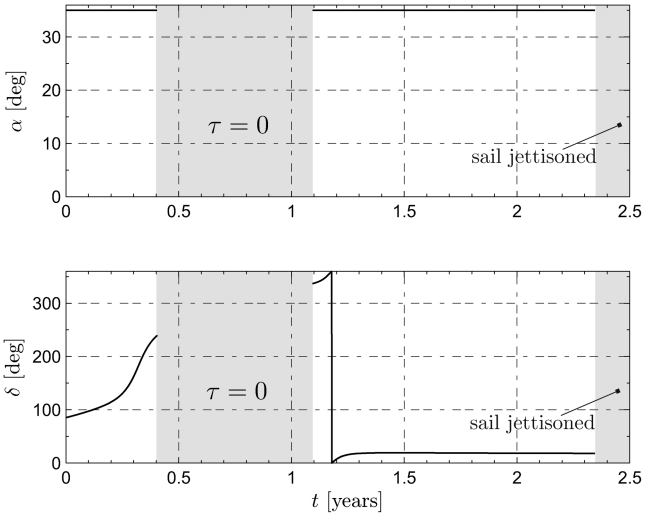

Fig. 25 Controls time histories for a mission toward the heliopause nose ($r_{\min} = 0.5$ AU and $a_\oplus = 2$ mm/s^2).

control variables (τ, α, and δ) are summarized in Fig. 25, in which the sail jettison distance ($r_c = 10$ AU) and the sailcraft initial angular position $\psi_0 \simeq 190$ deg are both highlighted.

Sailcraft Mass Budget

Having found the electric sail performance in terms of characteristic acceleration required to reach the heliopause nose within the prescribed interval (about 25 years), it is now necessary to investigate the corresponding requirements in terms of sailcraft mass budget for the IHP mission. In accordance with Lyngyi et al. [7], it is possible to subdivide ideally the sailcraft into two subsystems based on the two main operational phases: a spacecraft platform with total mass m_p, and an electric sail propulsion system with total mass m_E. Accordingly, the sailcraft in-flight initial total mass m_0 is given by

$$m_0 = m_p + m_E \tag{12}$$

Because the platform mass value is given, that is, $m_p = 213$ kg [40], the calculation of m_0 requires an estimate of m_E. To this end, it is advisable to use a mathematical model taken from [20], which allows one to obtain a reasonable approximation of the total mass of an electric sail spacecraft and of its characteristic acceleration. The model proposed in [20] is based on the preliminary plasma simulations performed by Janhunen, the electric sail inventor, and published in [18]. In the light of the currently available information, those plasma simulations seem to provide excessively conservative results. In fact, the propelling thrust obtainable by the electric sail depends on the number of electrons that are trapped by the potential structures of the tethers, because such electrons tend to shield the charged tethers and reduce their effect on the solar wind. Very recent studies have conjectured the existence of a natural mechanism that tends to remove the trapped electrons [41]. Using this new model, the electric sail thrust per unit length of tether (σ_F) is roughly 5 times higher than what was originally reported in [18]. A preliminary application example for the new thrust model is given in [39]. In particular, an electric sail comprising a total of $n = 100$ tethers, each one being of $l = 20$ km length, in an average solar wind is capable of developing a maximum propelling thrust $F = 1$ N at a solar distance of $r = r_\oplus$. In the example proposed in [39], the 20 kV charged tethers

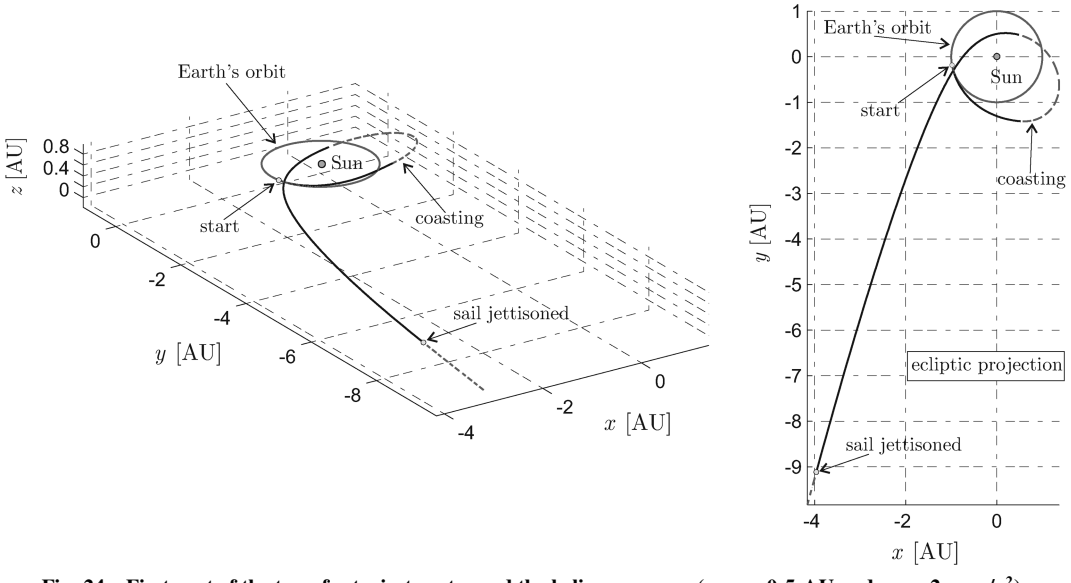

Fig. 24 First part of the transfer trajectory toward the heliopause nose ($r_{\min} = 0.5$ AU and $a_\oplus = 2$ mm/s^2).

have a total mass of $m_{\text{th}} = 11$ kg. With such a configuration, the electron gun requires $P = 400$ W power to operate. Using these data as a reference, it is possible to obtain a first-order estimate of the sailcraft mass distribution by suitably scaling the main contributions such as the electron gun power, the tethers total mass, and the propelling thrust. Let $L \triangleq nl = 2000$ km the total tethers length. Using the data from [39] one obtains

$$\sigma_F \triangleq \frac{F}{L} = 500 \ \frac{\text{nN}}{\text{m}}, \qquad \sigma_{m_{\text{th}}} \triangleq \frac{m_{\text{th}}}{L} = 5.5 \times 10^{-6} \ \frac{\text{kg}}{\text{m}}$$
$$\sigma_P \triangleq \frac{P}{L} = 2 \times 10^{-4} \ \frac{\text{W}}{\text{m}} \tag{13}$$

The numerical values for σ_F, $\sigma_{m_{\text{th}}}$, and σ_P that appear in Eq. (13) are treated as design data per unit tether length and will be used for estimating the total sailcraft mass of the IHP mission. In a preliminary mass breakdown calculation, the electric sail can be divided into three subsystems: the power system (with mass m_P), the tethers (with mass m_{th}), and all of the remaining elements that, for the sake of compactness, are comprised in the term structure (with mass m_s). The mass m_s includes, in addition to the sailcraft structural mass, the electron gun mass, the remote control mass, etc. Accordingly, the total mass of the electric sail can be written as

$$m_E = k_P \underbrace{\frac{\sigma_P L}{\eta}}_{m_P} + k_s \underbrace{(\sigma_{m_{\text{th}}} L}_{m_{\text{th}}} + m_s) \tag{14}$$

where now L, the total tethers length, is a design variable that must be calculated.

In Eq. (14) η is the specific power, that is, the power per mass unit associated to the power subsystem, while $k_P > 1$ and $k_s > 1$ are two dimensionless coefficients that model the uncertainty level (that is, the safety mass margins) in the definition of the sailcraft mass breakdown.

Taking into account the solar distance at which the sailcraft must operate, and in analogy to a similar choice for the platform [40], the best option for the power subsystem is represented by a radioisotope thermoelectric generator (RTG). Current RTGs [42] are characterized by a specific power of about 5 W/kg, but it is expected that in a near future the specific power may be increased up to 10 W/kg [7]. The currently estimated [40] specific power needed by the IHP platform is of about 10 W/kg.

Because of sufficiently good knowledge of RTG technology, assume a safety margin of 20%, that is, $k_P = 1.2$ in Eq. (14). On the other hand, the current scarce knowledge of the system details for the remaining parts of the electric sail implies a greater uncertainty level on k_s. A reasonable choice is to double the previous safety margin and assume, therefore, $k_s = 1.4$. To make a comparison, in the design of the IHP mission with a solar sail as the primary propulsion system, the safety margin was set equal to 20% [40].

Because the total electric sail thrust F at a distance of $r_\oplus$ is given by the product between the total length L and σ_F, from the definition of the characteristic acceleration, and taking into accounts Eqs. (12–14), the following relationship is obtained:

$$a_\oplus \triangleq \frac{F}{m_0} = \frac{\sigma_F L}{m_p + k_P \sigma_P L/\eta + k_s(\sigma_{m_{\text{th}}} L + m_s)} \tag{15}$$

Recalling Eq. (13) and (15) allows one to express the characteristic acceleration as a function of the three design parameters L, η, and m_s. Using the two values $\eta = (5, 10)$ W/kg, which correspond as stated to the current and near future technology level, it is possible to draw the function $a_\oplus = a_\oplus(L, m_s)$, as is shown in Fig. 26.

By comparing Figs. 26a and 26b, $a_\oplus$ and L being equal, an increase of the specific power from 5 to 10 W/kg would allow one to increase the structural mass of about 50 kg. Alternatively, m_s and $a_\oplus$ being equal (the latter value being given by the mission requirements, see Table 2), the increase in η translates into a reduction of the total tethers length. For an electric sail the value of L is roughly an index of the system complexity, as the reflecting surface is for a solar sail.

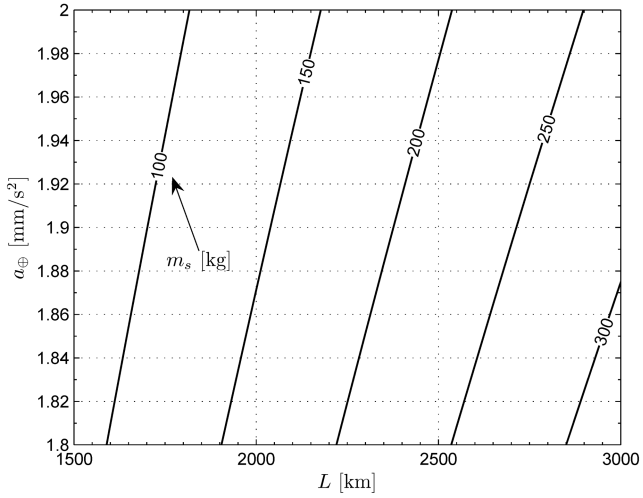

a) η = 5W/kg

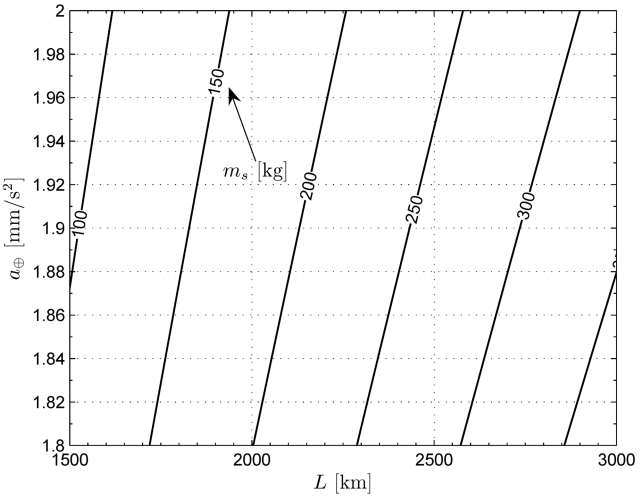

b) η = 10W/kg

Fig. 26 Characteristic acceleration as a function of total tethers length L and structure mass m_s.

Therefore, an increase of the specific power would be a very desirable result. However, the corresponding obtainable reduction in the tethers length, using the currently available values of $a_\oplus$, would not exceed 200–300 km, as is shown in Fig. 27, which corresponds to a percentage decrease of 10–15% with respect to the value of L required by this mission typology. Assuming $L = 2500$ km (that is, 25% greater than the value given in the example proposed in [39]), for each one of the three values of characteristic acceleration shown in Table 2, it is possible, with the aid of Eq. (15) and Fig. 26, to estimate the value of m_s and of the other sailcraft masses. The results of this

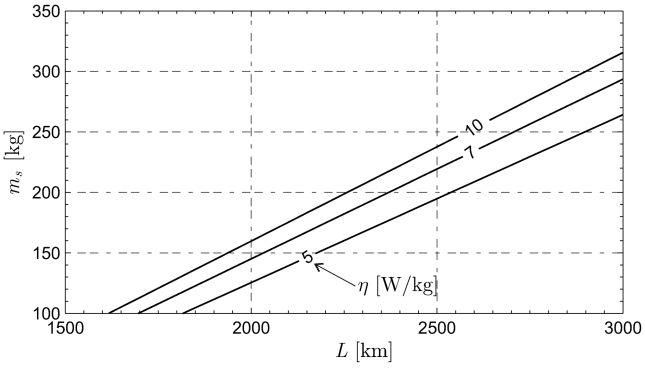

Fig. 27 Total tethers length L as a function of m_s and η for $a_\oplus$= 2 mm/s^2.

Table 3 Mass budget for missions toward the heliopause nose with $a_\oplus = (1.8, 1.9, 2)$ mm/s^2.

Mass	$a_\oplus = 1.8$ mm/s^2		$a_\oplus = 1.9$ mm/s^2		$a_\oplus = 2$ mm/s^2	
	$\eta = 5$ W/kg	$\eta = 10$ W/kg	$\eta = 5$ W/kg	$\eta = 10$ W/kg	$\eta = 5$ W/kg	$\eta = 10$ W/kg
m_p, kg	213	213	213	213	213	213
m_{th}, kg	13.75	13.75	13.75	13.75	13.75	13.75
m_P, kg	100	50	100	50	100	50
m_s, kg	244.4	287.3	218.3	261.2	194.9	237.7
m_0, kg with margins	694.44	694.44	657.9	657.9	625	625

calculation for $\eta = (5, 10)$ W/kg have been summarized in Table 3. Note that, once L is given, from the definition of σ_F the maximum propelling thrust at 1 AU is equal to $F = 1.25$ N. Table 3 shows that for all of the three cases the structure mass is comparable to that of the platform. If one thinks of the platform as a payload linked to the electric sail, the earlier mass breakdown shows that an IHP mission sailcraft can carry a payload mass fraction between 30 and 35%. For example, using the data from [40], an IHP mission having the same time length and performed with a square solar sail (spinning solar sail) may guarantee a payload mass fraction of 30% (40%), but requires a closer approach to the sun at a distance of 0.25 AU and a sailing mode time of about 5 years.

Note in passing that the earlier mass breakdown is conservative because the power needed by the electric sail, and, therefore, the mass m_P, was found by neglecting the power generation system of the platform. Actually the platform RTGs, capable of providing about 240 W at the beginning of their life [7], could be used in a redundancy mode during the sailing mode time in the interval $t \in [t_0, t_c]$.

Using an additional safety margin of 20% [7], from Table 3 the IHP sailcraft launch mass with electric sail option is between 750 and 834 kg, a value much less than the launch mass capability of the Soyuz-Fregat 2-1B, equal to 2000 kg (assuming an Earth escape with $C_3 = 0$). In particular, the solution with a Soyouz-Fregat 2-1B is identical to that conjectured for a mission scenario with a solar sail [7].

Conclusions

Missions toward the boundaries of the solar system have been studied for an electric sail, a spacecraft that uses the solar wind dynamic pressure for generating a continuous thrust without the need for reaction mass. Assuming a 2-D problem in which the orbital plane coincides with the ecliptic plane, minimum-time trajectories to reach a given solar distance have been studied in an optimal framework using an indirect approach. The optimal trajectory may or may not include a solar wind assist phase depending on the value of the sail characteristic acceleration. It is shown that the superiority of a direct transfer (that is, a trajectory that does not exploit the solar flyby) is confined to distances less than about 13 AU from the sun. Once the escape condition is met, the sail is jettisoned and the payload continues its mission using a flight by inertia. A medium-performance electric sail may reach a distance of 100 AU in about 15 years.

From the obtained results, the electric sail appears as an intriguing advanced propulsion system and a promising alternative to a solar sail. Moreover, it represents a realistic option for a complex and long term mission such as the IHP mission. Of course, the practical employment of this propulsion system requires the overcoming of several complex challenges, such as the deployment and control of 100 of about 20 km long tethers. The earlier simplified analysis of sailcraft mass budget has shown that the structure mass must remain below 300 kg to guarantee the fulfilment of the requirement concerning the value of sailcraft characteristic acceleration. However, the wide margin used in the analysis (equal to 40% for the structure mass) offers a reasonable trust that the structure mass constraint can be met.

Finally, note that in the earlier analysis the electric sail is used as a propulsion system external to the spacecraft platform. Such a choice is dictated by the need to obtain a reasonable comparison with the solar sail based solution, for which the study is available in the literature. However, assuming to integrate the payload suite (for which the mass is 20 kg only) within the electric sail and to redesign the whole power generation system in such a way to meet the sailcraft constraints during both the sailing mode time and the scientific mode, it would be possible to reduce significantly the in-flight total mass m_0 for a given value of $a_\oplus$. Clearly, this solution requires the presence of a suitable system for tethers release that must be engaged at the instant t_c. The detailed study of this solution, which is beyond the scope of this work, can be done when a detailed mass budget model of the various subsystems of the electric sail and a more refined model for the propelling thrust will be available.

Acknowledgment

The authors are indebted to Pekka Janhunen for his useful comments and background support.

References

[1] Stone, E. C., Cummings, A. C., McDonald, F. B., Heikkila, B. C., Lal, N., and Webber, W. R., "Voyager 1 Explores the Termination Shock Region and the Heliosheath Beyond," *Science*, Vol. 309, No. 5743, Sept. 2005, pp. 2017–2020. doi:10.1126/science.1117684

[2] Richardson, J. D., Kasper, J. C., Wang, C., Belcher, J. W., and Lazarus, A. J., "Cool Heliosheath Plasma and Deceleration of the Upstream Solar Wind at the Termination Shock," *Nature*, Vol. 454, No. 7200, July 2008, pp. 63–66. doi:10.1038/nature07024.

[3] Mewaldt, R. A., Kangas, J., Kerridge, S. J., and Neugebauer, M., "A Small Interstellar Probe to the Heliospheric Boundary and Interstellar Space,"*Acta Astronautica*, Vol. 35, No. suppliment, 1995, pp. 267–276. doi:10.1016/0094-5765(94)00192-O

[4] Sauer, C. G., Jr., "Solar Sail Trajectories for Solar Polar and Interstellar Probe Missions," AIAA Paper 99-336, Aug. 1999.

[5] Dachwald, B., "Optimal Solar Sail Trajectories for Missions to the Outer Solar System," *Journal of Guidance, Control, and Dynamics*, Vol. 28, No. 6, Nov.–Dec. 2005, pp. 1187–1193. doi:10.2514/1.13301

[6] Falkner, P., van de Berg, M. L., Renton, D., Atzei, A., Lyngvi, A., and Peacock, A., "Update on ESA's Technology Reference Studies," IAC Paper 05-A3.2A.07, 2005.

[7] Lyngvi, A. E., van den Berg, M. L., and Falkner, P., "Study Overview of the Interstellar Heliopause Probe," Vol. SCI-A/2006/114/IHP, No. 3, revision 4, ESA, Noordwijk, The Netherlands, April 2007, http://esagrid.esa.int/ science-e/www/object/index.cfm?fobjectid=40926 [retrieved 14 Oct. 2009].

[8] Dachwald, B., Macdonald, M., McInnes, C. R., Mengali, G., and Quarta, A. A., "Impact of Optical Degradation on Solar Sail Mission Performance," *Journal of Spacecraft and Rockets*, Vol. 44, No. 4, July–Aug. 2007, pp. 740–749. doi:10.2514/1.21432

[9] Dachwald, B., Mengali, G., Quarta, A. A., and Macdonald, M., "Parametric Model and Optimal Control of Solar Sails with Optical Degradation," *Journal of Guidance, Control, and Dynamics*, Vol. 29, No. 5, Sept.–Oct. 2006, pp. 1170–1178. doi:10.2514/1.20313

[10] Mengali, G., Quarta, A. A., Circi, C., and Dachwald, B., "Refined Solar Sail Force Model with Mission Application," *Journal of Guidance, Control, and Dynamics*, Vol. 30, No. 2, March–April 2007, pp. 512–520. doi:10.2514/1.24779

[11] Dachwald, B., "Solar Sail Performance Requirements for Missions to the Outer Solar System and Beyond," *55th International Astronautical Congress*, IAC Paper 04-S.P.11, Oct. 2004.

[12] Leipold, M., and Wagner, O., "'Solar Photonic Assist' Trajectory Design for Solar Sail Missions to the Outer Solar System and Beyond," *AAS/GSFC International Symposium on Space Flight Dynamics*, edited by T. H. Stengle, 98-386, Vol. 100, AAS, Greenbelt, MD, 1998, pp. 1031–1042.

[13] Winglee, R. M., Euripides, P., Ziemba, T., Slough, J., and Giersch, L., "Simulation of Mini- Magnetospheric Plasma Propulsion (M2P2) Interacting with an External Plasma Wind," *39th Joint Propulsion Conference and Exhibition*, AIAA Paper 2003-5225, July 2003.

[14] Winglee, R. M., Slough, J., Ziemba, T., and Goodson, A., "Mini-Magnetospheric Plasma Propulsion: Tapping the Energy of the Solar Wind for Spacecraft Propulsion," *Journal of Geophysical Research*, Vol. 105, No. A9, 2000, pp. 21,067–21,078. doi:10.1029/1999JA000334

[15] Mengali, G., and Quarta, A. A., "Optimal Missions with Minimagnetospheric Plasma Propulsion," *Journal of Guidance, Control, and Dynamics*, Vol. 29, No. 1, Jan.–Feb. 2006, pp. 209–212. doi:10.2514/1.18169

[16] Mengali, G., and Quarta, A. A., "Minimagnetospheric Plasma Propulsion for Outer Planet Missions," *Journal of Guidance, Control, and Dynamics*, Vol. 29, No. 5, Sept.–Oct. 2006, pp. 1239–1242. doi:10.2514/1.21634

[17] Janhunen, P., "Electric Sail for Spacecraft Propulsion," *Journal of Propulsion and Power*, Vol. 20, No. 4, 2004, pp. 763–764. doi:10.2514/1.8580

[18] Janhunen, P., and Sandroos, A., "Simulation Study of Solar Wind Push on a Charged Wire: Basis of Solar Wind Electric Sail Propulsion," *Annales Geophysicae*, Vol. 25, No. 3, 2007, pp. 755–767.

[19] Janhunen, P., "On the Feasibility of a Negative Polarity Electric Sail," *Annales Geophysicae*, Vol. 27, No. 4, 2009, pp. 1439–1447.

[20] Mengali, G., Quarta, A. A., and Janhunen, P., "Electric Sail Performance Analysis," *Journal of Spacecraft and Rockets*, Vol. 45, No. 1, Jan.–Feb. 2008, pp. 122–129. doi:10.2514/1.31769

[21] Mengali, G., Quarta, A. A., and Janhunen, P., "Considerations of Electric Sailcraft Trajectory Design," *Journal of the British Interplanetary Society*, Vol. 61, No. 8, Aug. 2008, pp. 326–329.

[22] Mengali, G., and Quarta, A. A., "Non-Keplerian Orbits for Electric Sails," *Celestial Mechanics and Dynamical Astronomy*, Vol. 105, Nos. 1-3, pp. 179–195, 2009. doi:10.1007/s10569-009-9200-y

[23] Janhunen, P., Mengali, G., and Quarta, A. A., "Electric Sail Propulsion Modeling and Mission Analysis," IEPC Paper 2007-352, Sept. 2007.

[24] Vulpetti, G., "Sailcraft at High Speed by Orbital Angular Momentum Reversal," *Acta Astronautica*, Vol. 40, No. 10, May 1997, pp. 733–758. doi:10.1016/S0094-5765(97)00153-7

[25] Wallace, R. A., Ayon, J. A., and Sprague, G. A., "Interstellar Probe Mission/System Concept," *Aerospace Conference Proceedings, 2000*, 53, Vol. 7, IEEE, Big Sky, MT, March 2000, pp. 385–396.

[26] Bryson, A. E., and Ho, Y. C., *Applied Optimal Control*, Hemisphere, New York, 1975, pp. 71–89.

[27] Lappas, V., Leipold, M., Lyngvi, A., Falkner, P., Fichtner, H., and Kraft, S., "Interstellar Heliopause Probe: System Design of a Solar Sail Mission to 200 AU," AIAA Paper 2005-6084, Aug. 2005.

[28] Leipold, M., Fichtner, H., Heber, B., Groepper, P., Lascar, S., Burger, F., Eiden, M., Niederstadt, T., Sickinger, C., Herbeck, L., Dachwald, B., and Seboldt, W., "Heliopause Explorer a Sailcraft Mission to the Outer Boundaries of the Solar System," *Acta Astronautica*, Vol. 59, Nos. 8–11, Oct.–Dec. 2006, pp. 785–796. doi:10.1016/j.actaastro.2005.07.024

[29] Leipold, M., "To the Sun and Pluto with Solar Sails and Micro-Sciencecraft," *Acta Astronautica*, Vol. 45, No. 4, Aug. 1999, pp. 549–555. doi:10.1016/S0094-5765(99)00175-7

[30] Mengali, G., and Quarta, A. A., "Optimal Three-Dimensional Interplanetary Rendezvous Using Nonideal Solar Sail," *Journal of Guidance, Control, and Dynamics*, Vol. 28, No. 1, Jan,–Feb. 2005, pp. 173–177. doi:10.2514/1.8325

[31] Bate, R. R., Mueller, D. D., and White, J. E., *Fundamentals of Astrodynamics*, Dover, New York, 1971, p. 429.

[32] Shampine, L. F., and Gordon, M. K., *Computer Solution of Ordinary Differential Equations: The Initial Value Problem*, W. H. Freeman, San Francisco, 1975, Chap. 10.

[33] Shampine, L. F., and Reichelt, M. W., "The MATLAB ODE Suite," *SIAM Journal on Scientific Computing*, Vol. 18, No. 1, Jan. 1997, pp. 1–22. doi:10.1137/S1064827594276424

[34] Sharma, D. N., and Scheeres, D. J., "Solar System Escape Trajectories Using Solar Sails," *Journal of Spacecraft and Rockets*, Vol. 41, No. 4, July–Aug. 2004, pp. 684–687. doi:10.2514/1.2354

[35] Macdonald, M., and McInnes, C. R., "Analytical Control Laws for Planet-Centered Solar Sailing," *Journal of Guidance, Control, and Dynamics*, Vol. 28, No. 5, Sept.–Oct. 2005, pp. 1038–1048. doi:10.2514/1.11400

[36] Macdonald, M., McInnes, C. R., and Dachwald, B., "Heliocentric Solar Sail Orbit Transfers with Locally Optimal Control Laws," *Journal of Spacecraft and Rockets*, Vol. 44, No. 1, Jan.–Feb. 2007, pp. 273–276. doi:10.2514/1.17297

[37] Mengali, G., and Quarta, A. A., "Near-Optimal Solar-Sail Orbit-Raising from Low Earth Orbit," *Journal of Spacecraft and Rockets*, Vol. 42, No. 5, Sept.–Oct. 2005, pp. 954–958. doi:10.2514/1.14184

[38] Mengali, G., and Quarta, A. A., "Earth Escape by Ideal Sail and Solar-Photon Thrustor Spacecraft," *Journal of Guidance, Control, and Dynamics*, Vol. 27, No. 6, Nov.–Dec, 2004, pp. 1105–1108. doi:10.2514/1.10637

[39] Janhunen, P., "Status Report of the Electric Sail—A Revolutionary Near-Term Propulsion Technique in the Solar System," *Sixth IAA Symposium on Realistic Near-Term Advanced Scientific Space Missions*, edited by G. Genta, IAA, Paris, 6–9 July 2009, pp. 49-54.

[40] Lyngvi, A., Falkner, P., Kemble, S., Leipold, M., and Peacock, A., "The Interstellar Heliopause Probe," *Acta Astronautica*, Vol. 57, Nos. 2–8, April 2005, pp. 104–111. doi:10.1016/j.actaastro.2005.03.042

[41] Janhunen, P., "Increased Electric Sail Thrust Through Removal of Trapped Shielding Electrons by Orbit Chaotisation Due to Spacecraft Body," *Annales Geophysicae*, Vol. 27, No. 8, 2009, pp. 3089–3100.

[42] Hunt, M. E., "High Efficiency Dynamic Radioisotope Power System for Space Exploration—A Status Report," *Aerospace and Electronic Systems Magazine*, Vol. 8, No. 12, 1993, pp. 18–23. doi:10.1109/62.246037.